

Questioning the Coverage-Length Metric in Conformal Prediction: When Shorter Intervals Are Not Better

Yizhou Min^{*†} Yizhou Lu^{*‡} Lanqi Li^{*†} Zhen Zhang[†] Jiaye Teng^{†§}

Abstract

Conformal prediction (CP) has become a cornerstone of distribution-free uncertainty quantification, conventionally evaluated by its coverage and interval length. This work critically examines the sufficiency of these standard metrics. We demonstrate that *the interval length might be deceptively improved through a counter-intuitive approach* termed Prejudicial Trick (PT), while the coverage remains valid. Specifically, for any given test sample, PT probabilistically returns an interval, which is either null or constructed using an adjusted confidence level, thereby preserving marginal coverage. While PT potentially yields a deceptively lower interval length, it introduces practical vulnerabilities: the same input can yield completely different prediction intervals across repeated runs of the algorithm. We formally derive the conditions under which PT achieves these misleading improvements and provide extensive empirical evidence across various regression and classification tasks. Furthermore, we introduce a new metric *interval stability* which helps detect whether a new CP method implicitly improves the length based on such PT-like techniques.

1 Introduction

Machine learning has been successfully applied in numerous fields. However, machine learning models often suffer from overconfidence issues (Guo et al., 2017; Minderer et al., 2021), making them unreliable for deployment in high-stakes areas such as medicine and finance (De Prado, 2018). Therefore, it is crucial to develop techniques for uncertainty quantification and calibrate the original model to enhance the reliability of predictions (Sullivan, 2015; Minderer et al., 2021; Smith, 2024).

Among all the uncertainty quantification methods, conformal prediction (CP) stands out due to its simplicity and distribution-free characteristics (Vovk et al., 2005; Shafer and Vovk, 2008; Angelopoulos and Bates, 2021). CP is a post hoc approach for constructing prediction intervals, based on a non-conformity score calculated on a hold-out calibration set (Algorithm 2). CP and its variants have demonstrated promising performances in numerous applications (Lei and Candès, 2021; Angelopoulos et al., 2022).

^{*}Equal Contribution

[†]Shanghai University of Finance and Economics

[‡]Fudan University

[§]Correspondence to tengjiaye@sufe.edu.cn

Algorithm 1 Prejudicial Trick (PT)

- 1: **Input:** conformal prediction algorithm (base) $\mathcal{A}_{1-\alpha}(\cdot; \hat{\mu})$, test point \mathbf{x}' , probability p .
- 2: Generate a uniform random variable $U \sim \text{Unif}([0, 1])$;
- 3: **if** $U > p$: **then**
- 4: Interval $\mathcal{C}_{1-\alpha}(\mathbf{x}') = \hat{\mu}(\mathbf{x}')$ (regression tasks) or $\mathcal{C}_{1-\alpha}(\mathbf{x}') = \emptyset$ (classification tasks);
- 5: **else**
- 6: Calculate the adjusted miscoverage rate $\alpha' = 1 - \frac{1-\alpha}{p}$;
- 7: Interval $\mathcal{C}_{1-\alpha}(\mathbf{x}') = \mathcal{A}_{1-\alpha'}(\mathbf{x}'; \hat{\mu})$;
- 8: **end if**
- 9: **Output:** Interval $\mathcal{C}_{1-\alpha}(\mathbf{x}')$.

Generally, researchers evaluate the intervals returned by CP via two criteria: *coverage* and *interval length*. Firstly, a valid coverage ensures that the actual response value has a high probability of falling within the interval. Secondly, the interval is encouraged to be as short as possible, as a shorter interval provides more precise information about prediction uncertainties. These two evaluation metrics are commonly used in the literature (Tibshirani et al., 2019; Teng et al., 2022; Angelopoulos et al., 2023; He and Lam, 2024) and a branch of works improves the length with several different meaningful approaches (Romano et al., 2019; Izbicki et al., 2020; Teng et al., 2022; Guan, 2023; Stutz et al., 2022). This raises a question on the potential risk of evaluating the CP methods narrowly on these standard metrics:

The key question:

If a new algorithm outperforms existing ones on coverage and length, should it automatically be considered superior for practical deployment?

Specifically, can a CP method maintain valid coverage and *deceptively improve interval length metrics* through counter-intuitive constructions, while *introducing practical risks*? Notably, this *differs* from the existing literature that proposes a new method that falls short in the length metric while performing better in the new metric (e.g., conditional coverage). To illustrate how it happens, we next consider the following Example 1:

Example 1 (The Pitfalls of Length.). Two doctors, Alice and Bob, are estimating recovery time for patients after treatment. CP with historical data reveals that 60% of patients recover within 4 years, and 80% within 5 years. When a new patient asks for an estimated recovery time, Alice and Bob adopt distinct strategies:

- Alice: Assign recovery time interval $[0, 4]$ years;
- Bob: Assign recovery time interval $[0, 5]$ with probability 0.75, while $[0, 0]$ with probability 0.25.

For both strategies in Example 1, 60% of patients fall in the estimated interval in expectation, thus satisfying the criteria for valid marginal coverage. Besides, Bob's approach yields a shorter average interval length $5 \times 75\% = 3.75 \ll 4$. Overall, Bob achieves a shorter interval while achieving the same coverage as Alice. However, Bob's strategy is flawed in its practical application, since (a) from the micro-level, Bob provides different intervals for the same patient if queried multiple times, and (b) from the macro-level, Bob randomly informs 25% of patients that they will recover immediately

after treatment regardless of their actual condition. The example is illustrated in Figure 3.

In this paper, inspired by the motivating example (Example 1), the *Prejudicial Trick* (PT) emerges as a practically invalid method that artificially shortens prediction intervals in CP (see Algorithm 1 and Figure 4). Instead of providing consistent intervals, PT assigns null intervals with a fixed probability to any test sample, and assigns confidence intervals with lower miscoverage rates in other cases to maintain the marginal coverage. While PT preserves marginal coverage and potentially reduces the average interval length, its rationale is less sound compared to standard methods like Vanilla Conformal Prediction (VCP). Specifically, PT suffers from two limitations:

- *Instability issues*: Repeated runs of PT produce different intervals for the same input;
- *Unfairness issues*: PT provides informative predictions for only a subset of test samples, while assigning uninformative null intervals to the rest¹.

From the theoretical perspective, we offer several theoretical results to provide deep understandings of PT regarding both coverage and length, and informally summarize them in Theorem 1.

Theorem 1 (Theorem Summary). *We term base as the base CP algorithm, term PT as the base algorithm with PT, and omit mild assumptions for clarity.*

For coverage, it holds that:

- PT satisfies marginal coverage guarantees under exchangeability assumptions (Theorem 6);
- PT guarantees conditional coverage if its base guarantees conditional coverage (Theorem 7);
- PT outperforms its base regarding the conditional coverage under some conditions, even if the base does not satisfy conditional coverage guarantees (Theorem 9).

For length, it holds that:

- PT achieves shorter average intervals than its base under some general conditions (Lemma 1);
- We provide sufficient conditions under which PT reduces the average interval length for both differentiable (Theorem 10) and non-differentiable (Corollary 3) length functions. Notably, these conditions are often satisfied in the common scenario of model misspecification (Remark 11).
- These results lead to corollaries for specific cases, such as when the length function is locally concave (Corollary 1) or when the base algorithm is VCP (Corollary 2).
- We also provide a failure case where PT cannot decrease the average length (Example 3).

From the experimental perspective, we verify our findings on various real-world datasets, regarding marginal and conditional coverage (Figure 1), and interval length (Table 2). Besides, we validate our findings under different settings, including different tasks (classification regimes in Table 4) and other CP algorithms (Conformalized Quantile Regression in Table 5).

However, the improvement on length is vacuous, as discussed in Section 3.5. To detect PT, We further introduce *Interval Stability*, a new metric to quantify the variation of the prediction for the same input over multiple runs. This metric is practically meaningful since it serves to identify and alert methods that implicitly or explicitly deploy invalid techniques like PT in the future (Remark 12).

¹In this paper, unfairness stems from the fact that a portion of samples are assigned null intervals in a run, even though each has an equal probability of being prejudiced. This differs from the unfairness concept grounded in conditional coverage (Zhao et al., 2020), where individuals are prejudiced based on their features.

Remark 2 (PT Hacks the Coverage-Length Metric). We present PT not as a practical solution, despite its theoretical advantages on the coverage-length metric. Instead, it serves as a **cautionary example that highlights issues such as instability and unfairness** during deployment. PT represents a simple way to *hack* the coverage-length metric. This reminds us of identifying where the actual improvements come from within a potentially complex algorithm, since they may implicitly contain PT-like tricks.

Remark 3 (Practical Relevance of the PT with Current CP Methods). PT reveals the danger of introducing randomness in CP methods. However, existing CP variants may implicitly introduce randomness. For example, localized CP (Hore and Barber, 2024) may require a machine learning model (trained with randomness) to estimate the uncertainty, and therefore, repeated runs may return different sets. If we cherry-pick the uncertainty estimator, by the results of PT, it always makes localized CP outperform VCP, even if the estimator does not contain the task information. We further discuss the relationship between PT and localized CP in Proposition 1. Moreover, some break-ties procedures (Stutz et al., 2022; Tyagi and Guo, 2023) introduce randomness (Table 8), which may bias or distort length measurements for such methods and may call for additional correction or more careful evaluation protocols.

Remark 4 (Why Study PT In Conformal Prediction). The relevance between PT and CP lies in the model misspecification (Remark 11). Specifically, model misspecification serves as a potential sufficient condition where PT works, and it generally appears in real-world applications of CP. However, the existence of model misspecification does not always hold for other interval estimation tasks, and therefore limits the extensions of PT beyond CP.

2 Related Work

Conformal prediction (Vovk et al., 2005) is mainly evaluated by the coverage-length metric. For coverage, CP provides finite sample guarantees under exchangeability assumptions (Vovk et al., 2005; Tibshirani et al., 2019; Barber et al., 2023), ensuring that prediction sets achieve the expected marginal coverage. Another related metric is conditional coverage, which is unachievable in finite sample settings without further assumptions (Vovk, 2012). Therefore, recent work focuses on various relaxations of conditional coverage (Barber et al., 2020; Gibbs et al., 2024).

Another metric is the average *interval length*, as shorter intervals are generally more informative (Lei et al., 2018; Sadinle et al., 2018). Numerous methods aim to construct adaptive intervals that reduce length while maintaining valid coverage. One line of work designs alternative non-conformity score functions: for example, Romano et al. (2019) integrate quantile regression, while Guan (2023) propose a localized method that adapts to test-time information. Other score functions have been proposed in (Feldman et al., 2021; Alaa et al., 2023; Han et al., 2022; Teng et al., 2022). Of particular interest is the method of Izbicki et al. (2020), which estimates the asymptotic conditional distribution of the non-conformity scores and constructs prediction intervals based on high-density regions. Another line of work involves a training procedure for interval-length optimization, such as CPL (Kiyani et al., 2024), CP-Gen (Bai et al., 2022), ConfTr (Stutz et al., 2022), and BoostedCP (Xie et al., 2024). Different from existing methods that provide principled and meaningful advances in CP, our proposed prejudicial trick achieves efficiency gains through an illusory construction, making the length improvement non-substantive.

Table 1: Results for the synthetic datasets (motivating example in Section 3.2). Comparison between VCP and PT-VCP under different α levels, regarding length and coverage.

α	p	VCP		PT-VCP	
		Coverage	Length	Coverage	Length
0.10	0.96	0.906 ± 0.004	22.894 ± 0.138	0.909 ± 0.005	22.614 ± 0.254
	0.98	0.906 ± 0.004	22.894 ± 0.138	0.904 ± 0.004	22.714 ± 0.165
0.20	0.96	0.792 ± 0.011	21.886 ± 0.125	0.799 ± 0.011	21.255 ± 0.136
	0.98	0.792 ± 0.011	21.886 ± 0.125	0.796 ± 0.010	21.589 ± 0.149

Besides coverage and length, several auxiliary metrics have been introduced. These include *excess* and *deficit* (Seedat et al., 2023), which measures the extent to which the prediction intervals are unnecessarily wide or insufficiently narrow; *false positive rate* (Fisch et al., 2022), which improves precision by limiting the number of incorrect labels in classification settings; and *conditional weighted coverage* (Jensen et al., 2024)—a hybrid metric that takes both coverage and length into account. Among them, a particularly important evaluation criterion is *group coverage* (Cauchois et al., 2021), which assesses the coverage and interval length across population subgroups defined by features or response magnitudes. However, in practice, people still tend to prioritize the coverage and length metrics (Lei et al., 2017; Cresswell et al., 2024; Zhang et al., 2024; Xu et al., 2025). Notably, this paper introduces a new metric distinct from existing approaches. Unlike existing studies that design metrics mainly to showcase favorable performance but often struggle with length, we show that PT potentially surpasses its base model in length while performing poorly under the new metric. We provide additional related works on CP and interval regression in Appendix A.2.

3 Prejudicial Trick with Deceptive Improvement

In this section, we challenge the coverage-length metric in CP by constructing a trick in Section 3.2. Specifically, this trick potentially improves the interval length while maintaining the coverage, yet it introduces instability and unfairness issues. We further investigate how this trick influences the coverage (Section 3.3) and the length (Section 3.4) theoretically and empirically. Finally, we discuss more details on the deceptive improvements of this trick in Section 3.5.

3.1 Preliminary

Conformal Prediction. CP creates statistically rigorous uncertainty sets for any predictive model. Given \mathbf{X} as the input and $\alpha \in (0, 1)$ as the miscoverage rate, CP returns an uncertainty set² $\mathcal{C}_{1-\alpha}(\mathbf{X})$ that satisfies

$$\mathbb{P}(y \in \mathcal{C}_{1-\alpha}(\mathbf{X})) \geq 1 - \alpha, \quad (1)$$

where y denotes the true response of feature \mathbf{X} . We omit the detailed discussion in Appendix A.4.

²CP algorithms either return a set measured by its size (for classification tasks), or return an interval measured by its length (for regression tasks). We do not distinguish between these terms throughout the paper.

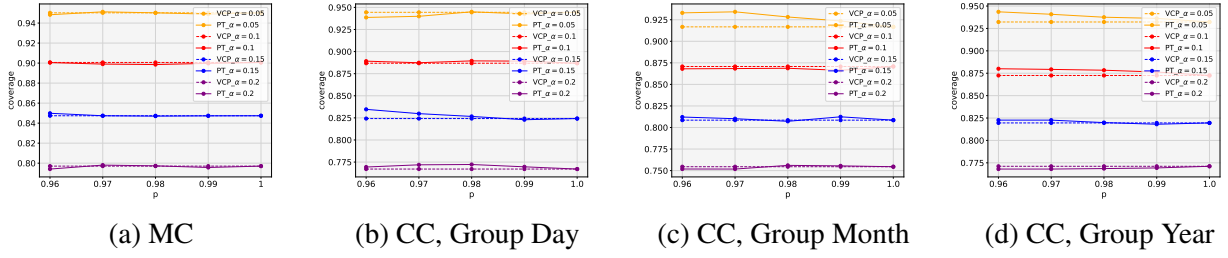


Figure 1: Comparing the (a) marginal coverage and (b, c, d) conditional coverage between VCP with and without PT. Results demonstrate that PT would not significantly change the marginal coverage; and PT has better conditional coverage compared to the base algorithm.

Notations. Let $\{Z_i\}_{i=1}^n$ denote n i.i.d. samples drawn from the distribution \mathcal{P}_Z , where $Z \in \mathbb{R}$. Denote $\{Z_{(i)}\}_{i=1}^n$ as the order statistics of $\{Z_i\}_{i=1}^n$ arranged in decreasing order, i.e., $Z_{(1)} \geq Z_{(2)} \geq \dots \geq Z_{(n)}$. The empirical τ -th quantile with n samples is defined as $\hat{Q}_\tau(\{Z_i\}_{i=1}^n) := Z_{(\lceil (n+1)(1-\tau) \rceil)}$. Let \emptyset denote the empty set, and $\mathbb{I}(\cdot)$ denote the indicator function. For a given set \mathcal{C} , let $|\mathcal{C}|$ denote the measure of the set. In this paper, we denote a trained CP algorithm that directly outputs the $1 - \alpha$ confidence interval given a test point as $\mathcal{A}_{1-\alpha}(\cdot; \hat{\mu})$ for simplicity, where $\hat{\mu}$ is the machine learning algorithm used in the CP algorithm.

3.2 Prejudicial Trick

In this section, we propose a trick (Algorithm 1) used in CP with the intuition from Example 1 and deploy this trick in a motivating example on a synthetic dataset. The experiment results in Table 1 demonstrate that this trick improves the interval length while maintaining the marginal coverage compared to its base. We begin with the construction process of this trick:

Construction Process. For each test point, assign a null set³ with probability $1 - p$, and assign the interval with an adjusted miscoverage rate $\alpha' = 1 - \frac{1-\alpha}{p}$ for the remaining p portion of test points, where $p \in (1 - \alpha, 1)$. Overall, for a new test point \mathbf{x}' , the interval is constructed as Equation (2):

$$\mathcal{C}_{1-\alpha}^{\text{PT}}(\mathbf{x}') = \begin{cases} \text{null set} & \text{with the probability } 1 - p, \\ \mathcal{C}_{1-\alpha'}^{\text{CP}}(\mathbf{x}') & \text{with the probability } p. \end{cases} \quad (2)$$

We call this process Prejudicial Trick (PT, see in Algorithm 1). Note that PT can be directly applied to any base CP algorithm. To illustrate that PT improves length without sacrificing marginal coverage, we empirically consider a motivating example in Example 2.

Example 2 (Synthetic Dataset). Consider a regression setting where the true underlying model is a linear model with the Gaussian mixture noise, given by $Y = \mathbf{X}^\top \boldsymbol{\beta} + \epsilon$, with $\mathbf{X} \sim \mathcal{N}(\mathbf{0}, I_2)$. The noise term ϵ follows $\mathcal{N}(\mu, 1)$ with probability 0.5, and $\mathcal{N}(-\mu, 1)$ with probability 0.5. The training fold, calibration fold, and test fold are generated based on this underlying distribution. We deploy VCP (Algorithm 2) and PT-VCP under such regimes. We refer to Appendix D.1.1 for more details.

³The null set represents a set of measure zero. It can be an empty set, or a single-point set in regression.

Results and Discussions of Example 2. Tabel 1 illustrates the results of Example 2, where *PT-VCP* improves the length while maintaining the marginal coverage compared to *VCP*. The results validate that the coverage-length metric could be hacked by invalid tricks like PT. The insights are as follows: the construction of ϵ guarantees $\mathcal{C}_{1-\alpha'}^{\text{CP}}$ close to $\mathcal{C}_{1-\alpha}^{\text{CP}}$ regarding the length when choosing proper α and p . Therefore, PT potentially improves the average length when averaging with those null sets.

Notably, Barber et al. (2020) propose a method similar to PT. Unlike PT which emphasizes the potential length improvement, Barber et al. (2020) mainly center on conditional coverage metrics. Moreover, we extend the scope of PT in Remark 5 by relaxing the notion of the null set.

Remark 5 (The extension of PT). PT in Algorithm 1 heavily relies on the notion of null sets. Fortunately, one can extend this null set with an interval returned by CP with a small coverage rate. For example, PT can be constructed as follows:

$$\mathcal{C}_{1-\alpha}^{\text{PT}}(\mathbf{x}') = \begin{cases} \mathcal{C}_{1-\alpha'_1}^{\text{CP}}(\mathbf{x}') & \text{with the probability } 1-p, \\ \mathcal{C}_{1-\alpha'_2}^{\text{CP}}(\mathbf{x}') & \text{with the probability } p, \end{cases} \quad (3)$$

where $(1-p)\alpha'_1 + p\alpha'_2 = \alpha$ which guarantees the marginal coverage and α'_1 is sufficiently small. We mainly consider the null set in this paper to simplify the related discussions.

Although PT appears to be an artificially constructed special case, we find that it strongly correlates with localized CP. We demonstrate that PT is a special case of localized CP in Proposition 1.

Proposition 1 (Relation Between PT And Localized CP). *In localized CP, we use the normalized nonconformity score to construct prediction sets, which is defined as*

$$\hat{S}^{\text{norm}}(x, y) = \hat{S}(x, y)/\hat{\sigma}(x), \quad (4)$$

where $\hat{S}(x, y)$ is the nonconformity score and $\hat{\sigma}(\cdot)$ is a trained estimator of local scale. Consider an extreme case that $\hat{\sigma}$ can only output 0^+ and 1 with probability $1-p$ and p respectively⁴. In this case, intervals returned by localized CP are equivalent to the form in Equation (2).

In practice, beyond the two-point distribution in Proposition 1, the interval length returned by localized CP across retraining runs might become a random variable following a more general distribution with a lower expectation. Consequently, even if one fixes a single trained $\hat{\sigma}$, retraining $\hat{\sigma}$ multiple times and reporting a favorable run amounts to cherry-picking, yielding shorter length without leveraging task information, while marginal coverage remains valid.

3.3 Coverage

This section investigates the coverage guarantee of CP with PT. We prove that PT maintains the marginal coverage guarantees (Theorem 6) and conditional coverage guarantees (Theorem 7, Theorem 9). The empirical validation in Figure 1 supports the theoretical findings.

Marginal Coverage. Theorem 6 proves that PT maintains the valid marginal coverage guarantees.

⁴If we train $\hat{\sigma}$ at each run, the randomness during training might lead to different outputs given a fixed x .

Theorem 6 (Marginal Coverage Guarantee). *Assume that the exchangeability assumption holds (see Proposition 3). Then the interval returned by Algorithm 1 with the adjusted miscoverage rate $\alpha' = 1 - \frac{1-\alpha}{p}$ guarantees that*

$$\mathbb{P}(y' \in \mathcal{C}_{1-\alpha}^{PT}(\mathbf{X}')) \geq 1 - \alpha, \quad (5)$$

where (\mathbf{X}', y') denotes a new test point.

The intuition behind Theorem 6: the null set (with probability $1 - p$) and the enlarged interval set with miscoverage α' (with probability p) reach the marginal coverage guarantees $p(1 - \alpha') = 1 - \alpha$.

Conditional Coverage. Theorem 7 further investigates the effect of PT on the condition coverage. Specifically, the returned interval $\mathcal{C}_{1-\alpha}^{PT}(\mathbf{X}')$ keeps the conditional coverage guarantees if the interval returned by its base algorithm $\mathcal{C}_{1-\alpha}^{CP}(\mathbf{X}')$ satisfies the conditional guarantees.

Theorem 7 (Conditional Coverage Guarantee). *Let $\mathcal{C}_{1-\alpha}^{CP}(\mathbf{X}')$ and $\mathcal{C}_{1-\alpha}^{PT}(\mathbf{X}')$ denote the returned interval of \mathbf{X}' respectively. If for any α , $\mathbb{P}(y \in \mathcal{C}_{1-\alpha}^{CP}(\mathbf{X}') \mid \mathbf{X}') \geq 1 - \alpha$ holds for \mathbf{X}' almost surely, then $\mathbb{P}(y \in \mathcal{C}_{1-\alpha}^{PT}(\mathbf{X}') \mid \mathbf{X}') \geq 1 - \alpha$ holds for any α and for \mathbf{X}' almost surely.*

The key insight behind Theorem 7: The randomness within PT is independent of the specific input. Therefore, such randomness is averaged out given a specific input, thus keeping the conditional coverage unchanged. Specifically, the conditional coverage is calculated as $p(1 - \alpha') = 1 - \alpha$.

Remark 8 (Comparison to the Tradeoffs between Conditional Coverage and Interval Length). Existing works on CP have analyzed the potential tradeoffs between conditional coverage and interval length (Barber et al., 2020; Gibbs et al., 2024). Our work differs from this line, since PT does not operate by creating such a trade-off. Specifically, Theorem 7 validates that PT does not violate the conditional coverage. See Section 3.5 for further discussions.

Theorem 7 requires that the base algorithm satisfies the conditional coverage guarantees. However, this requirement does not always hold in practice. We next prove in Theorem 9 that PT still exhibits the potential to outperform the base algorithm even when the requirement does not hold.

Theorem 9 (Sufficient Condition of Conditional Coverage Guarantees). *Let $f_{\mathcal{A}}(\alpha)$ denote the true conditional miscoverage rate within the subset \mathcal{A} , namely, $\mathbb{P}(y \in \mathcal{C}_{1-\alpha}^{CP}(\mathbf{X}) \mid \mathbf{X} \in \mathcal{A}) = 1 - f_{\mathcal{A}}(\alpha)$ where $\mathcal{C}_{1-\alpha}^{CP}(\mathbf{X})$ denotes the prediction set returned by the base algorithm. Define $\mathcal{F}(p) = p f_{\mathcal{A}}(1 - (1 - \alpha)/p)$ where $p \in (1 - \alpha, 1)$ represents the parameter in Algorithm 1. If $\mathcal{F}(\cdot)$ satisfies that $\mathcal{F}(1) - \mathcal{F}(p) \geq 1 - p$, then it holds that*

$$\mathbb{P}(y \in \mathcal{C}_{1-\alpha}^{PT}(\mathbf{X}) \mid \mathbf{X} \in \mathcal{A}) \geq \mathbb{P}(y \in \mathcal{C}_{1-\alpha}^{CP}(\mathbf{X}) \mid \mathbf{X} \in \mathcal{A}), \quad (6)$$

where $\mathcal{C}_{1-\alpha}^{CP}(\mathbf{X})$ denotes the prediction set returned by PT.

The key insight behind Theorem 9: The conditional miscoverage rate of PT arises from two probabilistic components. For the null set component, the miscoverage rate exceeds that of the base algorithm; for the other component, the miscoverage rate is lower. Therefore, by averaging these two components, PT potentially outperforms its base algorithm in terms of conditional coverage under certain conditions on the miscoverage function $f_{\mathcal{A}}(\alpha)$. Notably, Theorem 9 contains results on conditional coverages (for one-point set \mathcal{A}) and group coverages (for regular set \mathcal{A}).

Experiments. We compare marginal and conditional coverage rates returned with and without PT on BIKE dataset (Fanaee-T, 2013) using VCP (Algorithm 2) as the base algorithm. We omit the implementation details here and refer to Appendix D.2.2 for details. The results in Figure 1 demonstrate that (a) PT preserves the marginal coverage (Figure 1a); (b) When VCP fails to guarantee the group coverage, PT-VCP fails as well. Experimental results demonstrate that PT achieves comparable group coverage with its base models (Figure 1b, Figure 1c, Figure 1d). We provide more experiments on group coverage with different real-world datasets in Appendix C.1.

3.4 Length

This section investigates the sufficient conditions under which PT improves interval length while keeping the coverage unchanged, and further conducts experiments to validate the theoretical findings. We first propose Lemma 1 as a weak sufficient condition. We then derive a more informative condition under both differentiable regimes (Theorem 10) and non-differentiable regimes (Corollary 3). We further discuss the special cases on the local concave assumption (Corollary 1) and VCP regimes (Corollary 2), and find that misspecification usually satisfies the sufficient conditions (Remark 11). We finally present a failure case in Example 3 when PT cannot outperform its base regarding the interval length.

Experiment results on various datasets in Table 2 align closely with the theoretical results. Besides, we conduct experiments on classification tasks (Table 4), different base algorithms (Table 5), and conduct ablation studies on different hyperparameters (Figure 6-Figure 15).

Additional Notations. We introduce the following notations to facilitate the discussions in this section. Let α denote the miscoverage rate and $s(\mathbf{x}, y; \hat{\mu})$ denote the score function, where $\hat{\mu}(\cdot)$ denotes the learned model. Let $\mathcal{C}_{1-\alpha}^{\text{CP}}(\mathbf{x})$ denote the interval returned by CP at point \mathbf{x} , and $\mathcal{C}_{1-\alpha}^{\text{PT}}(\mathbf{x})$ denote the interval returned by its PT-variant (Algorithm 1). Let $\mathcal{L}(\mathbf{x}, 1 - \alpha; s)$ denote the length of the returned interval at point \mathbf{x} with miscoverage α , *i.e.*, $|\mathcal{C}_{1-\alpha}^{\text{CP}}(\mathbf{x})|$.

We next prove a series of sufficient conditions under which PT improves the interval length, starting from Lemma 1 which provides a straightforward sufficient condition.

Lemma 1 (General Sufficient Condition). *If \mathcal{L} satisfies the following condition, then there exists $p \in (1 - \tilde{\alpha}, 1)$ such that*

$$p\mathbb{E}\left(\mathcal{L}\left(\mathbf{x}, \frac{1 - \tilde{\alpha}}{p}; s\right)\right) < \mathbb{E}(\mathcal{L}(\mathbf{x}, 1 - \tilde{\alpha}; s)), \quad (7)$$

where $\tilde{\alpha}$ denotes the miscoverage rate and the expectation is taken over \mathbf{x} . Then the interval length returned by PT (with parameter p) outperforms that of its base algorithm,

$$\mathbb{E}|\mathcal{C}_{1-\tilde{\alpha}}^{\text{PT}}(\mathbf{X}')| < \mathbb{E}|\mathcal{C}_{1-\tilde{\alpha}}^{\text{CP}}(\mathbf{X}')|, \quad (8)$$

where the expectation is taken over the testing point \mathbf{X}' .

The intuition behind Lemma 1 is pretty simple: PT assigns null sets with a fixed probability whose measure is zero, thus potentially reducing the average length. Although the sufficient condition in Lemma 1 is general, the absence of additional assumptions makes it uninformative in practice. To obtain more insights, we next introduce a differentiable assumption in Theorem 10.

Table 2: Comparison of performance between VCP and PT-VCP in regression tasks across different datasets ($\alpha = 0.1$).

METHOD	BIAS	VCP		PT-VCP	
		COVERAGE	LENGTH	COVERAGE	LENGTH
MEPS-19	20	0.90 ± 0.000	42.34 ± 0.228	0.90 ± 0.000	41.92 ± 0.389
MEPS-20	20	0.90 ± 0.000	41.98 ± 0.116	0.90 ± 0.000	41.41 ± 0.241
MEPS-21	20	0.90 ± 0.004	42.28 ± 0.112	0.90 ± 0.000	41.90 ± 0.300
BIKE	10	0.90 ± 0.000	20.46 ± 0.018	0.90 ± 0.004	19.59 ± 0.018
BLOG-DATA	20	0.90 ± 0.004	41.67 ± 0.336	0.90 ± 0.000	41.13 ± 0.416
BIO	10	0.90 ± 0.004	21.13 ± 0.336	0.90 ± 0.000	20.44 ± 0.031
FACEBOOK-1	10	0.90 ± 0.000	20.81 ± 0.036	0.90 ± 0.000	20.80 ± 0.179
FACEBOOK-2	10	0.90 ± 0.000	20.97 ± 0.067	0.90 ± 0.000	21.01 ± 0.179
CONCRETE	5	0.90 ± 0.013	10.32 ± 0.009	0.89 ± 0.009	9.87 ± 0.031
STAR	5	0.91 ± 0.004	10.14 ± 0.004	0.91 ± 0.004	9.63 ± 0.027

Theorem 10 (First-order Condition). *Assume \mathcal{L} is first-order differentiable and satisfies*

$$\mathbb{E} \left(\frac{\mathcal{L}(\mathbf{x}, 1 - \tilde{\alpha}; s)}{1 - \tilde{\alpha}} \right) > \mathbb{E} \left(\frac{\partial}{\partial \alpha} \mathcal{L}(\mathbf{x}, \alpha; s) \Big|_{\alpha=1-\tilde{\alpha}} \right), \quad (9)$$

where $\tilde{\alpha}$ denotes the miscoverage rate and the expectation is taken over \mathbf{x} . Then there exists a parameter p in Algorithm 1, such that the interval length returned by PT outperforms that of its base algorithm, namely

$$\mathbb{E} |\mathcal{C}_{1-\tilde{\alpha}}^{PT}(\mathbf{X}')| < \mathbb{E} |\mathcal{C}_{1-\tilde{\alpha}}^{CP}(\mathbf{X}')|, \quad (10)$$

where the expectation is taken over the testing point \mathbf{X}' .

Theorem 10 follows the insights of Lemma 1, and further utilizes Equation 9 as the sufficient condition, which characterizes the local behavior of the interval length function. Theorem 10 provides more insights on when and how PT outperforms its base algorithm regarding the length metrics. We next derive a localized concave condition in Corollary 1 based on Theorem 10.

Corollary 1 (Localized Concave Conditions). *Under the settings in Theorem 10, the sufficient condition in Equation 9 holds if $\mathbb{E}(\mathcal{L}(\mathbf{x}, \alpha; s))$ is locally concave on $\alpha \in [0, 1 - \tilde{\alpha}]$.*

Corollary 1 provides a condition under which PT outperforms its base algorithm regarding length. Consider a regression problem with additive noise $y = f^*(x) + \epsilon$. If the noise distribution exhibits local concavity and the base model approximates the true function f^* well, then the length function $\mathbb{E}(\mathcal{L}(\mathbf{x}, \alpha; s))$ generally satisfies the localized concavity property. Consequently, the performance improvement of PT is guaranteed by Corollary 1. This inspires the construction of Example 2.

Besides, Corollary 2 focuses on the settings of deploying VCP. Since VCP returns the same length for each individual, the expectation operator in Theorem 10 degenerates.

Corollary 2 (Deterministic Case). *Under the settings in Theorem 10, if applying VCP (Algorithm 2)*

as the base algorithm, the sufficient condition in Equation 9 holds if

$$\frac{\mathcal{L}(\mathbf{x}, 1 - \tilde{\alpha}; s)}{1 - \tilde{\alpha}} > \frac{\partial}{\partial \alpha} \mathcal{L}(\mathbf{x}, \alpha; s) \Big|_{\alpha=1-\tilde{\alpha}}, \quad (11)$$

where the expectation operator degenerates due to the characteristics of VCP.

Unfortunately, real-world applications may not satisfy the differentiability assumption in Theorem 10. Therefore, we relax this assumption in Corollary 3.

Corollary 3 (Secant Sufficient Condition). *If there exists $u \in (1 - \tilde{\alpha}, 1)$, such that*

$$\frac{\mathbb{E}(\mathcal{L}(\mathbf{x}, 1 - \tilde{\alpha}; s))}{1 - \tilde{\alpha}} > \frac{\mathbb{E}(\mathcal{L}(\mathbf{x}, u; s)) - \mathbb{E}(\mathcal{L}(\mathbf{x}, 1 - \tilde{\alpha}; s))}{u - (1 - \tilde{\alpha})}, \quad (12)$$

where $\tilde{\alpha}$ denotes the miscoverage rate and the expectation is taken over \mathbf{x} . Then there exists a parameter $p = (1 - \tilde{\alpha})/u$ in Algorithm 1, such that the interval length returned by PT outperforms its base algorithm, namely,

$$\mathbb{E}|\mathcal{C}_{1-\tilde{\alpha}}^{\text{PT}}(\mathbf{X}')| < \mathbb{E}|\mathcal{C}_{1-\tilde{\alpha}}^{\text{CP}}(\mathbf{X}')|, \quad (13)$$

where the expectation is taken over the testing point \mathbf{X}' .

Corollary 3 shares similar intuitions with Theorem 10, and further relaxes the differentiability assumption by comparing the secant slopes. Informally, PT achieves smaller average lengths than its base algorithm when the length function does not grow extremely fast within the region $(1 - \tilde{\alpha}, 1)$.

Remark 11 (Relationship Between Misspecification and Sufficient Condition). Model misspecification is a common practical scenario that aligns with our theoretical analysis, as it typically satisfies the sufficient conditions in Theorem 10 and Corollary 3 (Wang and Blei, 2020; Huang et al., 2023). **Specifically, misspecification leads to a residual with a non-zero mean, resulting in a non-convex length function. This outcome is closely related to the local concavity condition in Corollary 1.** For this reason, we employ misspecification regimes in most of our experiments.

However, the aforementioned sufficient conditions are not always satisfied. We present a failure case in Example 3 and illustrate the empirical validation in Figure 5.

Example 3 (Failure Case). If the values of the non-conformity score in VCP follow a Gaussian distribution over randomness in \mathbf{x} , then for all $\alpha \in (0, 1)$, and all $p \in (1 - \alpha, 1)$, it holds that

$$\mathbb{E}|\mathcal{C}_{1-\alpha}^{\text{PT}}(\mathbf{X}')| > \mathbb{E}|\mathcal{C}_{1-\alpha}^{\text{CP}}(\mathbf{X}')|. \quad (14)$$

Example 3 demonstrates that PT does not always outperform its base algorithm regarding the coverage-length metric. However, our goal is not to present PT as a universally applicable method, but to demonstrate a risk in the coverage-length evaluation. To achieve this, the existence of any realistic scenarios where PT can create deceptively shorter intervals is sufficient.

Experiment. We conduct several experiments comparing the length returned with and without PT using VCP (Algorithm 2) on MEPS19-21 (Cohen et al., 2009), BIKE (Fanaee-T, 2013), BLOGDATA (Buza, 2014), BIO (Rana, 2013), FACEBOOK1-2 (Singh, 2015), CONCRETE (Yeh, 1998), STAR (Achilles et al., 2008). To simulate model misspecification, we manually add bias to the

label (as shown in the bias column in Table 2). We refer to Appendix D.2 for more details of the task settings. The results in Table 2 demonstrate that PT generally achieves smaller average lengths compared to its base algorithm in most cases (9 out of 10) while maintaining the coverage. Besides, we conduct more experiments and ablations:

- We compare the length of VCP and PT-VCP under classification tasks in Table 4;
- We use CQR (Romano et al., 2019) as the base algorithm on regression tasks in Table 5;
- We conduct ablation studies on hyperparameter p and misspecification level μ in Appendix C.2.

3.5 Deceptive Improvement

We prove that PT preserves (conditional) coverage guarantees in Section 3.3 and achieves shorter prediction intervals under certain conditions in Section 3.4. Despite these theoretical benefits, PT is poorly suited for practical deployment. The primary issue is that PT introduces randomness, causing prediction intervals to vary across different runs. This inherent instability undermines the method’s reliability. Besides, the problem becomes more dramatic in the scenario of Remark 5, where the individuals are grouped with different miscoverage rates. This randomness makes it impossible for a user to identify their assigned group, making the confidence interval meaningless. Therefore, **while PT may appear superior based on the traditional coverage-length metric, its practical instability makes it unsuitable for real-world deployment.** This discrepancy challenges the sufficiency of the coverage-length metric itself, suggesting it is not a complete measure of a method’s practical utility.

4 Interval Stability

In this section, we propose *interval stability* (Definition 1) which measures the randomness in each run of CP. We begin with the definition of interval stability.

Definition 1 (Interval Stability). *Let X denote a data point with returned confidence interval $C_{1-\alpha}(X)$, and let $|\cdot|$ denote a certain measure of the interval (e.g., its length). Let \mathcal{A} denote the CP algorithm, and \mathcal{D}_{ca} the calibration dataset. The interval stability is defined as*

$$IS(C_{1-\alpha}(X)) \triangleq \mathbb{E}_X [\text{Var}_{\mathcal{A}|X, \mathcal{D}_{ca}} (|C_{1-\alpha}(X)|)]. \quad (15)$$

The interval stability captures the expected variability of the interval size conditional on the test point and calibration randomness. Intuitively, it captures the inconsistency of the returned intervals when the algorithm is run multiple times on the same test point and calibration dataset.

Due to the stochastic nature of PT, it tends to produce a large interval stability, implying the practical instability issues. We prove in Proposition 2 that PT indeed introduces a non-zero interval stability.

Proposition 2. *Following the notations in Section 3.4, it holds that the interval stability is larger than zero:*

$$IS(C_{1-\alpha}^{PT}(X)) = p(1-p) \left(\mathbb{E} \left(\mathcal{L}(\mathbf{x}, \frac{1-\tilde{\alpha}}{p}; s) \right) \right)^2 > 0. \quad (16)$$

Notably, the *interval stability* metric is not just for detecting our specific PT construction, but serves as a safeguard to ensure that future advancements in CP are genuine and reliable, rather than arising from the unprincipled randomness. As the community pushes for shorter prediction intervals, there is a risk that increasingly complex methods might implicitly introduce randomness that offers deceptive gains. See Remark 12 for detailed discussions.

Remark 12 (Why Interval Stability). Interval stability is still meaningful even if existing approaches in CP do not always rely on randomness. In the existing literature, numerous approaches claim a superior performance through a smaller interval length, under the traditional coverage-length metric. In this paper, we show that randomness may break this metric through PT due to practical issues. This raises concerns that as methods become increasingly complex, they may implicitly utilize similar randomness to improve the length. Such effects may be unintended but hard to recognize. To address this issue, interval stability serves as a tool for detecting such issues and highlighting the risks inherent in the current reliance on the coverage-length metric alone.

Experiment. We follow the same setting as the experiment in Section 3.4, but use interval stability as the metric. Table 3 demonstrates that interval stability successfully detects the vacuous randomness in PT. We defer to Appendix C.1 for more experiments with CQR and classification regimes.

Notably, interval stability is zero for deterministic methods by design. The metric is not intended to replace coverage and length, but to complement them, acting as a specific check against the kind of vacuous randomness we identify. A value of zero is a *pass* on this specific test, confirming the method’s deterministic nature for a given input.

5 Conclusion

This paper demonstrates a potential risk of the coverage-length metric in CP. We introduce PT, a technique that hacks the conventional metric by producing deceptively shorter intervals while preserving coverage guarantees. However, PT relies on the randomness that leads to instability: the algorithm can produce different prediction sets for a given input on different runs. This creates practical issues in high-stakes scenarios. Our theoretical and empirical results confirm that while PT appears superior, its foundation is flawed. This discrepancy challenges the completeness of the coverage-length metric. Consequently, we propose Interval Stability as a diagnostic tool, which helps flag the potential vacuous randomness for a newly proposed method.

References

Chuan Guo, Geoff Pleiss, Yu Sun, and Kilian Q Weinberger. On calibration of modern neural networks. In *International conference on machine learning*, pages 1321–1330. PMLR, 2017.

Matthias Minderer, Josip Djolonga, Rob Romijnders, Frances Hubis, Xiaohua Zhai, Neil Houlsby, Dustin Tran, and Mario Lucic. Revisiting the calibration of modern neural networks. *Advances in Neural Information Processing Systems*, 34:15682–15694, 2021.

Marcos Lopez De Prado. *Advances in financial machine learning*. John Wiley & Sons, 2018.

Timothy John Sullivan. *Introduction to uncertainty quantification*, volume 63. Springer, 2015.

Ralph C Smith. *Uncertainty quantification: theory, implementation, and applications*. SIAM, 2024.

Vladimir Vovk, Alexander Gammerman, and Glenn Shafer. *Algorithmic learning in a random world*, volume 29. Springer, 2005.

Glenn Shafer and Vladimir Vovk. A tutorial on conformal prediction. *Journal of Machine Learning Research*, 9(3), 2008.

Anastasios N Angelopoulos and Stephen Bates. A gentle introduction to conformal prediction and distribution-free uncertainty quantification. *arXiv preprint arXiv:2107.07511*, 2021.

Lihua Lei and Emmanuel J Candès. Conformal inference of counterfactuals and individual treatment effects. *Journal of the Royal Statistical Society Series B: Statistical Methodology*, 83(5):911–938, 2021.

Anastasios N Angelopoulos, Amit Pal Kohli, Stephen Bates, Michael Jordan, Jitendra Malik, Thayer Alshaabi, Srigokul Upadhyayula, and Yaniv Romano. Image-to-image regression with distribution-free uncertainty quantification and applications in imaging. In *International Conference on Machine Learning*, pages 717–730. PMLR, 2022.

Ryan J Tibshirani, Rina Foygel Barber, Emmanuel Candes, and Aaditya Ramdas. Conformal prediction under covariate shift. *Advances in neural information processing systems*, 32, 2019.

Jiaye Teng, Chuan Wen, Dinghuai Zhang, Yoshua Bengio, Yang Gao, and Yang Yuan. Predictive inference with feature conformal prediction. *arXiv preprint arXiv:2210.00173*, 2022.

Anastasios N Angelopoulos, Stephen Bates, et al. Conformal prediction: A gentle introduction. *Foundations and Trends® in Machine Learning*, 16(4):494–591, 2023.

Shengyi He and Henry Lam. Statistically optimal uncertainty quantification for expensive black-box models. *arXiv preprint arXiv:2408.05887*, 2024.

Yaniv Romano, Evan Patterson, and Emmanuel Candes. Conformalized quantile regression. *Advances in neural information processing systems*, 32, 2019.

Rafael Izbicki, Gilson Shimizu, and Rafael Stern. Flexible distribution-free conditional predictive bands using density estimators. In *International Conference on Artificial Intelligence and Statistics*, pages 3068–3077. PMLR, 2020.

Leying Guan. Localized conformal prediction: A generalized inference framework for conformal prediction. *Biometrika*, 110(1):33–50, 2023.

David Stutz, Krishnamurthy, Dvijotham, Ali Taylan Cemgil, and Arnaud Doucet. Learning optimal conformal classifiers, 2022. URL <https://arxiv.org/abs/2110.09192>.

Shengjia Zhao, Tengyu Ma, and Stefano Ermon. Individual calibration with randomized forecasting, 2020. URL <https://arxiv.org/abs/2006.10288>.

Rohan Hore and Rina Foygel Barber. Conformal prediction with local weights: randomization enables local guarantees, 2024. URL <https://arxiv.org/abs/2310.07850>.

Chhavi Tyagi and Wenge Guo. Multi-label classification under uncertainty: A tree-based conformal prediction approach. In Harris Papadopoulos, Khuong An Nguyen, Henrik Boström, and Lars Carlsson, editors, *Proceedings of the Twelfth Symposium on Conformal and Probabilistic Prediction with Applications*, volume 204 of *Proceedings of Machine Learning Research*, pages 488–512. PMLR, 13–15 Sep 2023. URL <https://proceedings.mlr.press/v204/tyagi23a.html>.

Rina Foygel Barber, Emmanuel J Candès, Aaditya Ramdas, and Ryan J Tibshirani. Conformal prediction beyond exchangeability. *The Annals of Statistics*, 51(2):816–845, 2023.

Vladimir Vovk. Conditional validity of inductive conformal predictors. In Steven C. H. Hoi and Wray Buntine, editors, *Proceedings of the Asian Conference on Machine Learning*, volume 25 of *Proceedings of Machine Learning Research*, pages 475–490, Singapore Management University, Singapore, 04–06 Nov 2012. PMLR. URL <https://proceedings.mlr.press/v25/vovk12.html>.

Rina Foygel Barber, Emmanuel J. Candès, Aaditya Ramdas, and Ryan J. Tibshirani. The limits of distribution-free conditional predictive inference, 2020. URL <https://arxiv.org/abs/1903.04684>.

Isaac Gibbs, John J. Cherian, and Emmanuel J. Candès. Conformal prediction with conditional guarantees, 2024. URL <https://arxiv.org/abs/2305.12616>.

Jing Lei, Max G’Sell, Alessandro Rinaldo, Ryan J Tibshirani, and Larry Wasserman. Distribution-free predictive inference for regression. *Journal of the American Statistical Association*, 113(523):1094–1111, 2018.

Mauricio Sadinle, Jing Lei, and Larry Wasserman. Least ambiguous set-valued classifiers with bounded error levels. *Journal of the American Statistical Association*, 114(525):223–234, June 2018. ISSN 1537-274X. doi: 10.1080/01621459.2017.1395341. URL <http://dx.doi.org/10.1080/01621459.2017.1395341>.

Shai Feldman, Stephen Bates, and Yaniv Romano. Improving conditional coverage via orthogonal quantile regression. *Advances in neural information processing systems*, 34:2060–2071, 2021.

Ahmed M Alaa, Zeshan Hussain, and David Sontag. Conformalized unconditional quantile regression. In *International conference on artificial intelligence and statistics*, pages 10690–10702. PMLR, 2023.

Xing Han, Ziyang Tang, Joydeep Ghosh, and Qiang Liu. Split localized conformal prediction. *arXiv preprint arXiv:2206.13092*, 2022.

Shayan Kiyani, George Pappas, and Hamed Hassani. Length optimization in conformal prediction, 2024. URL <https://arxiv.org/abs/2406.18814>.

Yu Bai, Song Mei, Huan Wang, Yingbo Zhou, and Caiming Xiong. Efficient and differentiable conformal prediction with general function classes, 2022. URL <https://arxiv.org/abs/2202.11091>.

Ran Xie, Rina Foygel Barber, and Emmanuel J. Candès. Boosted conformal prediction intervals, 2024. URL <https://arxiv.org/abs/2406.07449>.

Nabeel Seedat, Alan Jeffares, Fergus Imrie, and Mihaela van der Schaar. Improving adaptive conformal prediction using self-supervised learning, 2023. URL <https://arxiv.org/abs/2302.12238>.

Adam Fisch, Tal Schuster, Tommi Jaakkola, and Dr. Regina Barzilay. Conformal prediction sets with limited false positives. In Kamalika Chaudhuri, Stefanie Jegelka, Le Song, Csaba Szepesvari, Gang Niu, and Sivan Sabato, editors, *Proceedings of the 39th International Conference on Machine Learning*, volume 162 of *Proceedings of Machine Learning Research*, pages 6514–6532. PMLR, 17–23 Jul 2022. URL <https://proceedings.mlr.press/v162/fisch22a.html>.

Vilde Jensen, Filippo Maria Bianchi, and Stian Normann Anfinsen. Ensemble conformalized quantile regression for probabilistic time series forecasting. *IEEE Transactions on Neural Networks and Learning Systems*, 35(7):9014–9025, July 2024. ISSN 2162-2388. doi: 10.1109/tnnls.2022.3217694. URL <http://dx.doi.org/10.1109/TNNLS.2022.3217694>.

Maxime Cauchois, Suyash Gupta, and John C Duchi. Knowing what you know: valid and validated confidence sets in multiclass and multilabel prediction. *Journal of machine learning research*, 22(81):1–42, 2021.

Jing Lei, Max G’Sell, Alessandro Rinaldo, Ryan J. Tibshirani, and Larry Wasserman. Distribution-free predictive inference for regression, 2017. URL <https://arxiv.org/abs/1604.04173>.

Jesse C. Cresswell, Yi Sui, Bhargava Kumar, and Noël Vouitsis. Conformal prediction sets improve human decision making, 2024. URL <https://arxiv.org/abs/2401.13744>.

Dongping Zhang, Angelos Chatzimparmpas, Negar Kamali, and Jessica Hullman. Evaluating the utility of conformal prediction sets for ai-advised image labeling, 2024. URL <https://arxiv.org/abs/2401.08876>.

Yunpeng Xu, Mufang Ying, Wenge Guo, and Zhi Wei. Two-stage risk control with application to ranked retrieval, 2025. URL <https://arxiv.org/abs/2404.17769>.

Hadi Fanaee-T. Bike Sharing. UCI Machine Learning Repository, 2013. DOI: <https://doi.org/10.24432/C5W894>.

Yixin Wang and David M. Blei. Variational bayes under model misspecification, 2020. URL <https://arxiv.org/abs/1905.10859>.

Daolang Huang, Ayush Bharti, Amauri Souza, Luigi Acerbi, and Samuel Kaski. Learning robust statistics for simulation-based inference under model misspecification, 2023. URL <https://arxiv.org/abs/2305.15871>.

Joel W. Cohen, Steven B. Cohen, and Jessica S. Banthin. The medical expenditure panel survey: A national information resource to support healthcare cost research and inform policy and practice. *Medical Care*, 47:S44–S50, 2009.

Krisztian Buza. Feedback prediction for blogs. In *Data analysis, machine learning and knowledge discovery*, pages 145–152. Springer, 2014.

Prashant Rana. Physicochemical Properties of Protein Tertiary Structure. UCI Machine Learning Repository, 2013. DOI: <https://doi.org/10.24432/C5QW3H>.

Kamaljot Singh. Facebook Comment Volume. UCI Machine Learning Repository, 2015. DOI: <https://doi.org/10.24432/C5Q886>.

I-Cheng Yeh. Concrete Compressive Strength. UCI Machine Learning Repository, 1998. DOI: <https://doi.org/10.24432/C5PK67>.

CM Achilles, Helen Pate Bain, Fred Bellott, Jayne Boyd-Zaharias, Jeremy Finn, John Folger, John Johnston, and Elizabeth Word. Tennessee’s student teacher achievement ratio (star) project. *Harvard Dataverse*, 1:2008, 2008.

Rina Foygel Barber, Emmanuel J Candes, Aaditya Ramdas, and Ryan J Tibshirani. The limits of distribution-free conditional predictive inference. *Information and Inference: A Journal of the IMA*, 10(2):455–482, 2021.

Harris Papadopoulos, Alex Gammerman, and Volodya Vovk. Normalized nonconformity measures for regression conformal prediction. In *Proceedings of the IASTED International Conference on Artificial Intelligence and Applications (AIA 2008)*, pages 64–69, 2008.

Anastasios Angelopoulos, Stephen Bates, Jitendra Malik, and Michael I Jordan. Uncertainty sets for image classifiers using conformal prediction. *arXiv preprint arXiv:2009.14193*, 2020.

Lahav Dabah and Tom Tirer. On calibration and conformal prediction of deep classifiers. *arXiv preprint arXiv:2402.05806*, 2024.

Jiaye Teng, Zeren Tan, and Yang Yuan. T-sci: A two-stage conformal inference algorithm with guaranteed coverage for cox-mlp. In *International conference on machine learning*, pages 10203–10213. PMLR, 2021.

Emmanuel Candès, Lihua Lei, and Zhimei Ren. Conformalized survival analysis. *Journal of the Royal Statistical Society Series B: Statistical Methodology*, 85(1):24–45, 2023.

Jing Lei, Alessandro Rinaldo, and Larry Wasserman. A conformal prediction approach to explore functional data. *Annals of Mathematics and Artificial Intelligence*, 74:29–43, 2015.

Niccolò Ajroldi, Jacopo Diquigiovanni, Matteo Fontana, and Simone Vantini. Conformal prediction bands for two-dimensional functional time series. *Computational Statistics & Data Analysis*, 187:107821, 2023.

Soroush H Zargarbashi, Simone Antonelli, and Aleksandar Bojchevski. Conformal prediction sets for graph neural networks. In *International Conference on Machine Learning*, pages 12292–12318. PMLR, 2023.

Soroush H Zargarbashi and Aleksandar Bojchevski. Conformal inductive graph neural networks. *arXiv preprint arXiv:2407.09173*, 2024.

Chen Xu and Yao Xie. Conformal prediction interval for dynamic time-series. In *International Conference on Machine Learning*, pages 11559–11569. PMLR, 2021.

Kamile Stankeviciute, Ahmed M Alaa, and Mihaela van der Schaar. Conformal time-series forecasting. *Advances in neural information processing systems*, 34:6216–6228, 2021.

Ying Jin, Zhimei Ren, and Emmanuel J Candès. Sensitivity analysis of individual treatment effects: A robust conformal inference approach. *Proceedings of the National Academy of Sciences*, 120(6):e2214889120, 2023.

Yuya Sasaki, Takuya Ura, and Yichong Zhang. Unconditional quantile regression with high-dimensional data. *Quantitative Economics*, 13(3):955–978, 2022.

Volodymyr Kuleshov, Nathan Fenner, and Stefano Ermon. Accurate uncertainties for deep learning using calibrated regression. In *International conference on machine learning*, pages 2796–2804. PMLR, 2018.

Kang Wang and Subhashis Ghosal. Coverage of credible intervals in bayesian multivariate isotonic regression. *The Annals of Statistics*, 51(3):1376–1400, 2023.

Jiri Navratil, Matthew Arnold, and Benjamin Elder. Uncertainty prediction for deep sequential regression using meta models. *arXiv preprint arXiv:2007.01350*, 2020.

Harris Papadopoulos, Vladimir Vovk, and Alex Gammerman. Regression conformal prediction with nearest neighbours. *Journal of Artificial Intelligence Research*, 40:815–840, 2011.

Jia Deng, Wei Dong, Richard Socher, Li-Jia Li, K. Li, and Li Fei-Fei. Imagenet: A large-scale hierarchical image database. *2009 IEEE Conference on Computer Vision and Pattern Recognition*, pages 248–255, 2009.

Appendix

We firstly restate our contributions and demonstrate some additional related works, extended discussions, omitted preliminary and illustrations in Appendix A. Then we provide missing proofs in Appendix B. In Appendix C, we illustrate the omitted experimental results. In Appendix D, we present implementation details of our experiments.

A Additional Details and Discussion

A.1 Contributions Restatement

We summarize our contributions as follows:

- We observe that the traditional coverage-length criteria in conformal prediction might be hacked using a counter-intuitive method PT, (Algorithm 1), since PT might deceptively improve the length while maintaining the coverage but raises fairness issues;
- We theoretically derive in Lemma 1 the conditions under which PT deceptively improves length, while keeping valid marginal coverage (Theorem 6) and conditional coverage (Theorem 7, Theorem 9). We further derive several sufficient conditions under which PT improves length with first-order differentiability assumption (Theorem 10) or without first-order differentiability assumption (Corollary 3);
- We propose a new metric in Section 4, termed interval stability. Interval stability measures the variance of the prediction interval over the input introduced by the conformal prediction algorithms, helping to mitigate the adverse impacts of PT.

A.2 Additional Related Works

Conformal prediction. Conformal prediction is a post hoc calibration framework that constructs statistically rigorous uncertainty sets for predictions from machine learning models (Vovk et al., 2005; Shafer and Vovk, 2008; Lei et al., 2018; Foygel Barber et al., 2021; Angelopoulos and Bates, 2021; Papadopoulos et al., 2008). Traditionally, vanilla conformal prediction is deployed in regression tasks (Vovk et al., 2005; Shafer and Vovk, 2008; Lei et al., 2018). Later, a branch of research expands vanilla conformal prediction to diverse data structures and applications, including classification tasks (Angelopoulos et al., 2020; Dabah and Tirer, 2024), censored data in survival analysis (Teng et al., 2021; Candès et al., 2023), functional data (Lei et al., 2015; Ajroldi et al., 2023), graph-based models (Zargarbashi et al., 2023; Zargarbashi and Bojchevski, 2024), time series data (Xu and Xie, 2021; Stankeviciute et al., 2021), treatment effects (Lei and Candès, 2021; Jin et al., 2023), *etc.*

Interval regression. While coverage guarantees and interval length serve as fundamental metrics for evaluating conformal prediction (Vovk et al., 2005; Lei et al., 2018; Barber et al., 2020), these criteria are deeply entrenched in the broader paradigm of interval regression methodologies. Established approaches including quantile regression (Alaa et al., 2023; Sasaki et al., 2022) and

Bayesian credible intervals (Kuleshov et al., 2018; Wang and Ghosal, 2023) similarly prioritize the dual metrics. Of particular relevance is Navratil et al. (2020) who proposes an excess and deficit metrics beyond the traditional coverage-length metric. Our paper differs from Navratil et al. (2020) in that our main contributions center on uncovering the inherent limitations of coverage-length metrics. Additionally, we contend that the proposed excess and deficit metrics cannot be directly applied to PT-VCP.

A.3 More Discussions

Similarity between PT and method discussed in Barber et al. (2020). In Section 3.2, we mention the similarity between our PT method and the randomness discussed in Barber et al. (2020). While the mechanism in our work bears a structural resemblance to that in Barber et al. (2020), our motivation and conclusion are fundamentally different. Barber et al. (2020) investigate the inherent trade-offs required to achieve conditional coverage, using randomization as a tool to explore theoretical limits. In contrast, our work focuses on the evaluation paradigm itself. We use PT not to achieve a desirable property (like conditional coverage), but to demonstrate a failure mode of a widely-used metric (average interval length). Our primary contribution is to highlight this pitfall and propose a remedy (Interval Stability), a direction not explored by Barber et al. (2020).

A.4 Omitted Preliminary

Interval Prediction. Interval prediction aims to construct a confidence interval that contains the true response value with a user-specified probability. Compared to traditional point estimation, interval prediction provides more comprehensive statistical information by quantifying the uncertainty using the interval length, which is often a more challenging goal. Definition 2 presents the formal definition.

Definition 2 (Interval Prediction). *Let (\mathbf{X}, Y) denote a feature-response pair. Given a miscoverage rate α , interval prediction aims to construct a confidence interval $\mathcal{C}_{1-\alpha}(\mathbf{X})$, such that*

$$\mathbb{P}(Y \in \mathcal{C}_{1-\alpha}(\mathbf{X})) \geq 1 - \alpha. \quad (17)$$

Given the coverage in Equation (17), a smaller confidence interval indicates a more precise estimate.

Conformal Prediction. To construct an interval prediction, we introduce a widely used approach called vanilla conformal prediction. The VCP method is typically divided into four stages: dataset splitting, training, calibration, and construction. The whole procedure is presented in Algorithm 2.

Dataset Splitting. Let $\mathcal{D} = \{(\mathbf{x}_i, y_i) : i \in \mathcal{I}\}$ denote the i.i.d. samples from a distribution \mathcal{P}_{XY} over the covariate $\mathbf{X} \in \mathbb{R}^d$ and the response $Y \in \mathbb{R}$. The VCP first randomly splits the dataset \mathcal{D} into two folds: a training fold $\mathcal{D}_{\text{tr}} = \{(\mathbf{x}_i, y_i) : i \in \mathcal{I}_{\text{tr}}\}$ and a calibration fold $\mathcal{D}_{\text{ca}} = \{(\mathbf{x}_i, y_i) : i \in \mathcal{I}_{\text{ca}}\}$, where $\mathcal{I}_{\text{tr}} \cup \mathcal{I}_{\text{ca}} = \mathcal{I}$ and $\mathcal{I}_{\text{tr}} \cap \mathcal{I}_{\text{ca}} = \emptyset$.

Training Process. We train a model denoted by $\hat{\mu}(\cdot)$ (e.g., a neural network) via the training fold \mathcal{D}_{tr} .

Calibration Process. Given the trained model $\hat{\mu}(\cdot)$, VCP calculates the non-conformity score on the calibration fold \mathcal{D}_{ca} , denoted by $\mathcal{V} = \{s(\mathbf{x}_i, y_i; \hat{\mu}) : i \in \mathcal{I}_{\text{ca}}\}$. The non-conformity score $s(\cdot)$

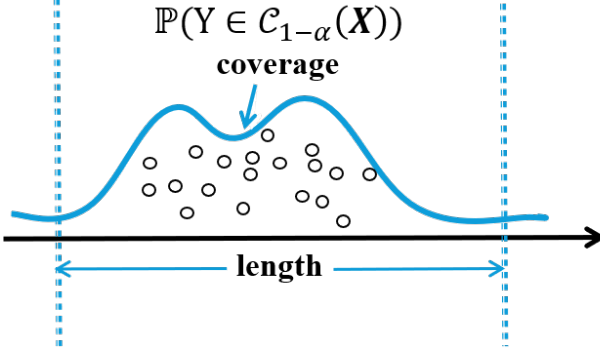


Figure 2: Illustration of coverage and interval length.

measures how well the model $\hat{\mu}(\cdot)$ fits the ground truth. A commonly used non-conformity score in regression tasks is the absolute residual, defined as $s(\mathbf{x}_i, y_i; \hat{\mu}) = |y_i - \hat{\mu}(\mathbf{x}_i)|$.

Construction Process. Finally, for a given miscoverage rate α , we then compute a $(1 - \tilde{\alpha})$ -th quantile $\hat{Q}_{1-\tilde{\alpha}}(\mathcal{V})$ of the empirical distribution of the non-conformity score set \mathcal{V} calculated on the calibration set, where $1 - \tilde{\alpha} = (1 - \alpha)(1 + 1/|\mathcal{V}|)$. The prediction interval at a new point \mathbf{x}' is then given by

$$\mathcal{C}_{1-\alpha}(\mathbf{x}') = \{y : s(\mathbf{x}', y; \hat{\mu}) \leq \hat{Q}_{1-\tilde{\alpha}}(\mathcal{V})\}. \quad (18)$$

Coverage and Length. To evaluate the performance of interval prediction, two commonly used metrics: *coverage* and *length* are defined in Definition 3, as further illustrated in Figure 2.

Definition 3 (Coverage and Length). *Let (\mathbf{X}, Y) denote a feature-response pair from a joint distribution \mathcal{P}_{XY} , and let $\mathcal{C}_{1-\alpha}(\mathbf{X})$ denote the confidence interval to be evaluated and let $|\cdot|$ denote a certain measure of $\mathcal{C}_{1-\alpha}(\mathbf{X})$. The coverage and length of $\mathcal{C}_{1-\alpha}(\mathbf{X})$ is given by:*

$$\begin{aligned} \text{Coverage} &:= \mathbb{E} [\mathbb{I}(Y \in \mathcal{C}_{1-\alpha}(\mathbf{X}))], \\ \text{Length} &:= \mathbb{E} |\mathcal{C}_{1-\alpha}(\mathbf{X})|. \end{aligned} \quad (19)$$

For example, the length of the prediction interval given by VCP in Equation (18) is:

$$\text{Length} = \mathbb{E} [2\hat{Q}_{1-\tilde{\alpha}}(\mathcal{V})]. \quad (20)$$

Notably, the two metrics in Definition 3 evaluate the quality of prediction intervals from different perspectives. Figure 2 illustrates the coverage and length given a distribution. Firstly, high coverage ensures that the true value falls within the interval with high probability. A valid confidence interval should guarantee that the coverage exceeds $1 - \alpha$, as suggested in Equation 17. However, setting a sufficiently large interval always guarantees Equation (17), which is impractical and meaningless. Therefore, the length metric is required to ensure the interval's precision. Based on the above discussion, the gold standard in conformal prediction is *making the length as small as possible, given that the coverage is larger than $1 - \alpha$* .

Following the gold standard, VCP ensures the coverage guarantee under mild exchangeability assumption (Proposition 3), but pays less attention to the length. As a result, numerous works on

improving the length of VCP from different perspectives (Papadopoulos et al., 2011; Romano et al., 2019) use intuitively valid approaches.

Proposition 3 (Coverage Guarantee). *The terms \mathcal{U}_i are exchangeable if arbitrary permutation leads to the same distribution, i.e., $(\mathcal{U}_1, \dots, \mathcal{U}_{|\mathcal{I}_{ca}|+1}) \stackrel{d}{=} (\mathcal{U}_{\pi(1)}, \dots, \mathcal{U}_{\pi(|\mathcal{I}_{ca}|+1)})$ with arbitrary permutation π over $1, \dots, |\mathcal{I}_{ca}|+1$, where $\stackrel{d}{=}$ denotes equivalence in distribution. Suppose that the data pair $(\mathbf{x}_i, y_i), i \in \mathcal{I}_{ca}$ and the test point (\mathbf{x}', y') are exchangeable, then the confidence interval $\mathcal{C}_{1-\alpha}(\mathbf{x}')$ returned by Algorithm 2 satisfies*

$$\mathbb{P}(y' \in \mathcal{C}_{1-\alpha}(\mathbf{x}')) \geq 1 - \alpha.$$

A.5 Missing Illustration

In this section, we present the missing illustration of Example 1 in Section 1, the illustration of PT (Figure 4) and VCP algorithm mentioned in Section 3.1.

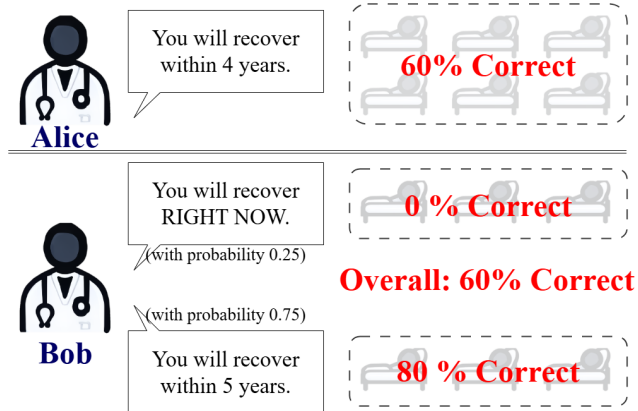


Figure 3: Illustration of Example 1. Doctor Alice and Bob both achieve 60% accuracy. Bob is more precise regarding length, but the corresponding strategy is not practically valid.

Algorithm 2 Vanilla Conformal Prediction (VCP)

- 1: **Input:** miscoverage rate α , dataset $\mathcal{D} = \{(\mathbf{x}_i, y_i) : i \in \mathcal{I}\}$, test point \mathbf{x}' , non-conformity score function $s(\mathbf{x}_i, y_i; \hat{\mu})$.
- 2: Randomly split \mathcal{D} into a training fold $\mathcal{D}_{tr} = \{(\mathbf{x}_i, y_i) : i \in \mathcal{I}_{tr}\}$ and a calibration fold $\mathcal{D}_{ca} = \{(\mathbf{x}_i, y_i) : i \in \mathcal{I}_{ca}\}$;
- 3: Train a model $\hat{\mu}$ based on the training fold \mathcal{D}_{tr} ;
- 4: Calculate the non-conformity score on the calibration fold \mathcal{D}_{ca} , denoted by $\mathcal{V} = \{s(\mathbf{x}_i, y_i, \hat{\mu}) : i \in \mathcal{I}_{ca}\}$;
- 5: Compute the $(1 - \tilde{\alpha})$ -th quantile $\hat{Q}_{1-\tilde{\alpha}}(\mathcal{V})$ of the empirical distribution of the non-conformity score set \mathcal{V} calculated on the calibration set \mathcal{D}_{ca} , where $1 - \tilde{\alpha} = (1 - \alpha)(1 + 1/|\mathcal{V}|)$;
- 6: **Output:** Interval $\mathcal{C}_{1-\alpha}(\mathbf{x}') = \{y : s(\mathbf{x}', y; \hat{\mu}) \leq \hat{Q}_{1-\tilde{\alpha}}(\mathcal{V})\}$.

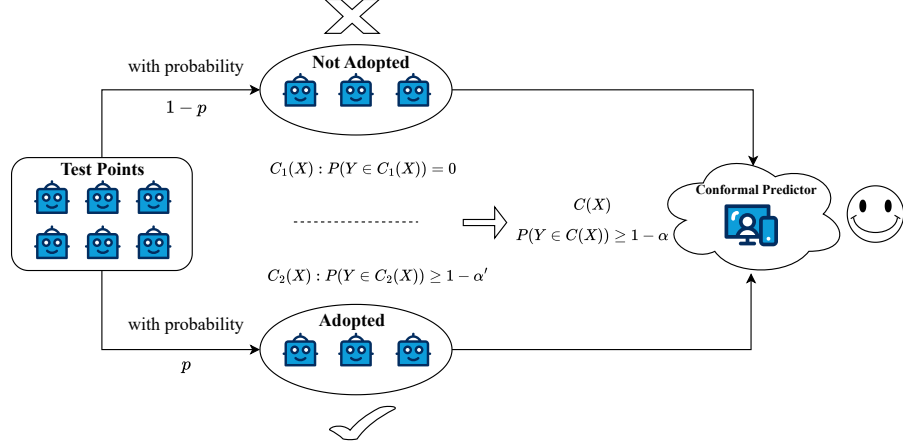


Figure 4: The illustration of Prejudicial Trick (PT). To obtain a $1 - \alpha$ confidence interval, PT first assigns empty sets for a $1 - p$ subset of the test points, and assigns $1 - \alpha'$ confidence interval for the remaining test points where $\alpha' < \alpha$. The returned confidence interval still satisfies $\mathbb{P}(Y \in \mathcal{C}(X)) \geq 1 - \alpha$ by setting a proper α' .

B Proofs for Theorems and Corollaries

B.1 Proof of Theorem 6

The returned interval could be in two folds: the vacuous fold and the meaningful fold. Therefore, by the definition of PT (Algorithm 1), we have

$$\mathbb{P}(y' \in \mathcal{C}_{1-\alpha}^{PT}(\mathbf{X}')) = \mathbb{P}(y' \in \mathcal{C}_{1-\alpha'}^{CP}(\mathbf{X}') \mid \mathcal{C}_{1-\alpha'}^{CP}(\mathbf{X}') \text{ is in the meaningful fold})p \quad (21)$$

$$+ \mathbb{P}(y' \in \mathcal{C}_{1-\alpha'}^{CP}(\mathbf{X}') \mid \mathcal{C}_{1-\alpha'}^{CP}(\mathbf{X}') \text{ is in the vacuous fold})(1 - p) \quad (22)$$

$$\geq (1 - \alpha')p = 1 - \alpha. \quad (23)$$

B.2 Proof of Theorem 7

Given that for all possible values of \mathbf{X} , there holds

$$\mathbb{P}(y \in \mathcal{C}_{1-\alpha}^{CP}(\mathbf{X}) \mid \mathbf{X}) \geq 1 - \alpha \quad (24)$$

holds almost surely, we have

$$\mathbb{P}(y' \in \mathcal{C}_{1-\alpha}^{PT}(\mathbf{X}') \mid \mathbf{X}) = \mathbb{P}(y' \in \mathcal{C}_{1-\alpha'}^{CP}(\mathbf{X}') \mid \mathcal{C}_{1-\alpha'}^{CP}(\mathbf{X}') \text{ is in the meaningful fold, } \mathbf{X})p \quad (25)$$

$$+ \mathbb{P}(y' \in \mathcal{C}_{1-\alpha'}^{CP}(\mathbf{X}') \mid \mathcal{C}_{1-\alpha'}^{CP}(\mathbf{X}') \text{ is in the vacuous fold, } \mathbf{X})(1 - p) \quad (26)$$

$$\geq (1 - \alpha')p = 1 - \alpha \quad (27)$$

holds almost surely.

B.3 Proof of Theorem 9

Given that it holds

$$\mathbb{P}(y \in \mathcal{C}_{1-\alpha}^{CP}(\mathbf{X}) \mid \mathbf{X} \in \mathcal{A}) = 1 - f_{\mathcal{A}}(\alpha), \quad (28)$$

we have

$$\mathbb{P}(y \in \mathcal{C}_{1-\alpha}^{PT}(\mathbf{X}) \mid \mathbf{X} \in \mathcal{A}) = p(1 - f_{\mathcal{A}}(\alpha')), \quad (29)$$

where $\alpha' = 1 - (1 - \alpha)/p$. And we have

$$\mathcal{F}(1) - \mathcal{F}(p) = f_{\mathcal{A}}(\alpha) - pf_{\mathcal{A}}\left(1 - \frac{1-\alpha}{p}\right) \geq 1 - p \quad (30)$$

$$\Rightarrow p\left(1 - f_{\mathcal{A}}\left(1 - \frac{1-\alpha}{p}\right)\right) \geq 1 - f_{\mathcal{A}}(\alpha) \quad (31)$$

$$\Rightarrow p(1 - f_{\mathcal{A}}(\alpha')) \geq 1 - f_{\mathcal{A}}(\alpha). \quad (32)$$

Therefore, we have

$$\mathbb{P}(y \in \mathcal{C}_{1-\alpha}^{PT}(\mathbf{X}) \mid \mathbf{X} \in \mathcal{A}) \geq \mathbb{P}(y \in \mathcal{C}_{1-\alpha}^{CP}(\mathbf{X}) \mid \mathbf{X} \in \mathcal{A}). \quad (33)$$

B.4 Proof of Lemma 1

By the definition of \mathcal{L} and PT in Algorithm 1, when the returned set belongs to the meaningful fold, the length is $\mathcal{L}(\mathbf{x}, (1 - \tilde{\alpha})/p; s)$, given the non-conformity score function and miscoverage rate $\tilde{\alpha}$. And the length of the returned set belongs to the vacuous fold is 0. Therefore, the expected length of the set returned by PT is

$$p\mathbb{E}\left(\mathcal{L}\left(\mathbf{x}, \frac{1-\tilde{\alpha}}{p}; s\right)\right), \quad (34)$$

where the expectation is taken over \mathbf{x} . Then we get the general sufficient condition is

$$\exists p \in (1 - \tilde{\alpha}, 1) \quad s.t. \quad p\mathbb{E}\left(\mathcal{L}\left(\mathbf{x}, \frac{1-\tilde{\alpha}}{p}; s\right)\right) < \mathbb{E}(\mathcal{L}(\mathbf{x}, 1 - \tilde{\alpha}; s)). \quad (35)$$

B.5 Proof of Theorem 10

Let $\mathcal{G}(c) = \mathbb{E}(\mathcal{L}(\mathbf{x}, 1 - \tilde{\alpha}; s))$, the sufficient condition in Lemma 1 is

$$\exists p \in (c, 1), \quad s.t. \quad p\mathcal{G}(c/p) < \mathcal{G}(c). \quad (36)$$

Note that when $p = 1$, $p\mathcal{G}(c/p) = \mathcal{G}(c)$, the sufficient condition of Eq (36) is

$$\mathcal{F}'(1) > 0, \quad \text{where } \mathcal{F}(p) = p\mathcal{G}(c/p), \quad (37)$$

which is equivalent to

$$\frac{\mathcal{G}(c)}{c} > \mathcal{G}'(c) \Rightarrow \mathbb{E}\left(\frac{\mathcal{L}(\mathbf{x}, 1 - \tilde{\alpha}; s)}{1 - \tilde{\alpha}}\right) > \mathbb{E}\left(\left.\frac{\partial}{\partial \alpha} \mathcal{L}(\mathbf{x}, \alpha; s)\right|_{\alpha=1-\tilde{\alpha}}\right). \quad (38)$$

B.6 Proof of Corollary 3

Use the notation in Appendix B.5, the general sufficient condition could be written as

$$\exists p \in (c, 1), \text{ s.t. } p\mathcal{G}(c/p) < \mathcal{G}(c). \quad (39)$$

If there exists $u \in (1 - \tilde{\alpha})$ satisfies

$$\frac{\mathcal{G}(c)}{c} > \frac{\mathcal{G}(u) - \mathcal{G}(c)}{u - c}, \quad (40)$$

we have

$$\frac{c}{u}\mathcal{G}(u) < \mathcal{G}(c). \quad (41)$$

Let $p = c/u$, we have

$$p\mathcal{G}(c/p) < \mathcal{G}(c). \quad (42)$$

Eq (40) is actually the condition

$$\frac{\mathbb{E}(\mathcal{L}(\mathbf{x}, 1 - \tilde{\alpha}; s))}{1 - \tilde{\alpha}} > \frac{\mathbb{E}(\mathcal{L}(\mathbf{x}, u; s)) - \mathbb{E}(\mathcal{L}(\mathbf{x}, 1 - \tilde{\alpha}; s))}{u - (1 - \tilde{\alpha})}. \quad (43)$$

B.7 Proof of Example 3

When the non-conformity score follows a Gaussian distribution, the analytical solutions of the interval length returned by VCP and PT-VCP are

$$|\mathcal{C}_{1-\tilde{\alpha}}^{VCP}(\mathbf{X}')| = 2\Phi^{-1}\left(1 - \frac{\tilde{\alpha}}{2}\right), \quad |\mathcal{C}_{1-\tilde{\alpha}}^{PT}(\mathbf{X}')| = 2p\Phi^{-1}\left(1 - \frac{1}{2}\left(1 - \frac{1-\tilde{\alpha}}{p}\right)\right) \quad (44)$$

where $\Phi(\cdot)$ is the cumulative distribution function of the Gaussian distribution. Therefore, PT fails since Lemma 2.

Lemma 2. $\forall \alpha \in (0, 1), p \in (1 - \alpha, 1)$, there holds

$$\Phi^{-1}\left(1 - \frac{\tilde{\alpha}}{2}\right) < p\Phi^{-1}\left(1 - \frac{1}{2}\left(1 - \frac{1-\tilde{\alpha}}{p}\right)\right) \quad (45)$$

Proof. Using the symmetry identity $\Phi^{-1}(1 - u) = -\Phi^{-1}(u)$, the desired inequality is equivalent to

$$p\Phi^{-1}\left(\frac{1}{2}\left(1 - \frac{1-\alpha}{p}\right)\right) < \Phi^{-1}(\alpha/2). \quad (46)$$

Define

$$u_0 := \alpha/2 \in (0, 1/2), \quad u(p) := \frac{1}{2}\left(1 - \frac{1-\alpha}{p}\right) \in (0, 1/2). \quad (47)$$

Let $g(u) := \Phi^{-1}(u)$ on $(0, 1/2)$. Since

$$g'(u) = \frac{1}{\phi(\Phi^{-1}(u))} > 0, \quad g''(u) = \frac{\Phi^{-1}(u)}{\phi(\Phi^{-1}(u))^2} < 0, \quad (48)$$

Table 3: Comparison between VCP and VCP with PT regarding interval stability.

Method	meps-19	meps-20	meps-21	bike	blog-data	bio	facebook-1	facebook-2	concrete	star
VCP	0.00 \pm 0.000									
PT-VCP	1.26 \pm 0.015	1.24 \pm 0.008	1.26 \pm 0.011	0.58 \pm 0.002	1.23 \pm 0.014	0.61 \pm 0.001	0.62 \pm 0.005	1.19 \pm 0.006	1.14 \pm 0.012	1.14 \pm 0.007

where $\phi(\cdot)$ denotes the p.d.f. of the standard normal distribution, the function g is increasing and strictly concave. Hence, for any $u \leq u_0$,

$$g(u) \leq g(u_0) + g'(u_0)(u - u_0). \quad (49)$$

Plugging $u = u(p)$ into Eq (49) and multiplying both sides by $p \in (0, 1)$ gives

$$p g(u(p)) \leq p g(u_0) + p g'(u_0)(u(p) - u_0). \quad (50)$$

A direct calculation yields

$$u(p) - u_0 = \frac{(1 - \alpha)(p - 1)}{2p} < 0. \quad (51)$$

Subtracting $g(u_0)$ from both sides of Eq (50) and using Eq (51), we obtain

$$p g(u(p)) - g(u_0) \leq (1 - p) \left[-g(u_0) + \frac{1 - \alpha}{2\phi(g(u_0))} \right]. \quad (52)$$

Here $1 - p > 0$. Moreover, since $g(u_0) = \Phi^{-1}(\alpha/2) < 0$ and $\phi(g(u_0)) > 0$, the bracket in Eq (52) is nonnegative. Thus the right-hand side of Eq (52) is nonpositive, implying

$$p g(u(p)) - g(u_0) < 0, \quad (53)$$

which is exactly inequality Eq (46). The inequality is strict because $u(p) \neq u_0$ and g is strictly concave.

Reverting to the upper-tail form via $\Phi^{-1}(1 - u) = -\Phi^{-1}(u)$ completes the proof:

$$\Phi^{-1}(1 - \alpha/2) < p \Phi^{-1}\left(\frac{1}{2}\left(1 + \frac{1-\alpha}{p}\right)\right). \quad (54)$$

□

C Omitted Experiments

In this section, we present all the omitted experiments. In Appendix C.1, we demonstrate the missing experimental results in Section 3.3 and Section 3.4. In Appendix C.2, we exhibit the ablation study results.

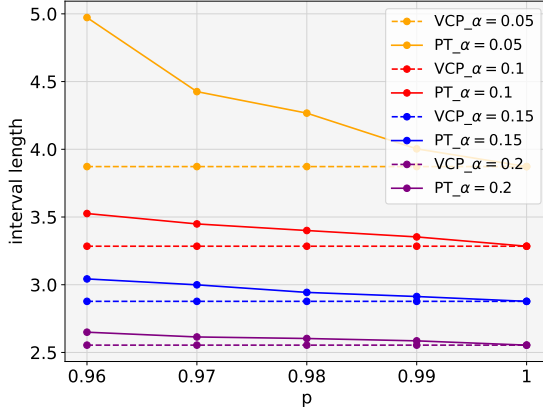


Figure 5: PT fails to improve length when the conditions on the distribution of non-conformity score are not satisfied.

Table 4: Comparison between VCP and PT-VCP in classification tasks across different models. Experiments on RAPS ($\alpha = 0.1, p = 0.95$), with index range chosen as 300.

METHOD	BIAS	VCP		PT-VCP	
		MODEL	COVERAGE	LENGTH	COVERAGE
RESNET18	40	0.90 ± 0.000	304.02 ± 0.004	0.90 ± 0.000	295.60 ± 0.233
RESNET50	40	0.90 ± 0.000	302.09 ± 0.027	0.90 ± 0.000	290.29 ± 0.224
RESNET101	40	0.90 ± 0.000	302.01 ± 0.004	0.90 ± 0.000	289.56 ± 0.174
RESNET152	40	0.89 ± 0.004	301.53 ± 0.054	0.90 ± 0.000	288.98 ± 0.165
RESNEXT101	40	0.90 ± 0.000	301.48 ± 0.013	0.90 ± 0.000	288.49 ± 0.201
VGG16	40	0.90 ± 0.004	303.39 ± 0.143	0.90 ± 0.000	293.34 ± 0.304
SHUFFLENET	40	0.90 ± 0.000	304.05 ± 0.040	0.90 ± 0.000	295.79 ± 0.282
INCEPTION	40	0.90 ± 0.000	304.10 ± 0.013	0.90 ± 0.000	297.25 ± 0.228
DENSENET161	40	0.90 ± 0.000	302.03 ± 0.009	0.90 ± 0.000	289.29 ± 0.197

C.1 Omitted Experimental Results

Classification Tasks. We extend PT to classification tasks. We apply PT to the real-world IMAGENET-VAL dataset (Deng et al., 2009) with several pre-trained models, a similar setting with Angelopoulos et al. (2020). To simulate model misspecification, a bias is introduced to the logits of several classes before the softmax operation. The magnitude of the bias is determined based on the scale of the outputs. The experimental results on classification tasks in Table 4 perform similarly to regression tasks. Specifically, PT-VCP attains valid coverage across different models (Theorem 6) while improving the length compared to VCP (Corollary 3).

Conformalized Quantile Regression. We deploy PT into other variants of conformal prediction. Specifically, we choose CQR as a baseline (Romano et al., 2019). CQR inherits the advantages of both conformal prediction and classical quantile regression. We use the same datasets and evaluation metrics as in Section 3.4. To mimic the model misspecification, we add bias directly to the lower and upper quantiles obtained by the quantile regression. The experimental results on the real-world

Table 5: Comparison between CQR and PT-CQR in quantile regression task across different datasets.

Method	Bias	CQR		PT-CQR	
		Coverage	Length	Coverage	Length
Dataset					
meps-19	1	0.91 ± 0.000	4.60 ± 0.148	0.91 ± 0.246	4.44 ± 0.143
meps-20	1	0.91 ± 0.000	4.58 ± 0.192	0.91 ± 0.179	4.41 ± 0.188
meps-21	1	0.91 ± 0.000	4.65 ± 0.080	0.91 ± 0.161	4.52 ± 0.107
bike	1	0.91 ± 0.000	2.61 ± 0.013	0.90 ± 0.268	2.51 ± 0.009
blog-data	1	0.91 ± 0.000	3.80 ± 0.107	0.93 ± 0.116	3.61 ± 0.098
bio	1	0.91 ± 0.000	3.45 ± 0.009	0.90 ± 0.112	3.32 ± 0.009
facebook-1	1	0.91 ± 0.000	3.38 ± 0.022	0.92 ± 0.125	3.22 ± 0.027
facebook-2	1	0.91 ± 0.000	3.57 ± 0.027	0.92 ± 0.085	3.39 ± 0.027
concrete	2	0.91 ± 0.000	4.39 ± 0.022	0.88 ± 0.648	4.23 ± 0.018
star	2	0.91 ± 0.000	4.15 ± 0.004	0.90 ± 0.349	3.96 ± 0.009

CQR tasks are exhibited in Table 5. It illustrates that *PT achieves shorter interval length while maintaining valid coverage on CQR*.

Group Coverage. In Section 3.3, we conduct experiments to evaluate the different performance of VCP and PT-VCP regarding group coverage. The experimental results shown in Table 6 demonstrate that PT not only achieves shorter confidence intervals while maintaining overall coverage, *but also improves the group coverage in regression tasks*⁵.

Interval Stability. In Section 4, we introduce a new evaluation criterion, termed *interval stability* and conduct several empirical evaluations using the datasets described in Section 3.4, the results of which are listed in Table 3. We further investigate the performance of the interval stability metric using CQR as the base algorithm in Table 7. The results are similar to the results in Table 3. We also evaluate the interval stability metric on classification tasks. As shown in Table 8, interval stability successfully identify the vacuous randomness in PT.

C.2 Ablation Studies

This section exhibits the ablation studies on the probability hyperparameter p in PT and the bias parameter μ on different base algorithms (Figure 6-Figure 15). All the experiments are conducted based on various miscoverage rates α . The experiment results demonstrate that, although not all the probability hyperparameters p outperform the base algorithm, our goal is to show that *there exist multiple (at least one) probability hyperparameters such that PT-VCP outperforms VCP, which suffices to challenge the coverage-length gold standard*. Furthermore, we find that the bias parameter actually matters here, implying that PT-VCP performs better than VCP under misspecification, which validates Corollary 3.

⁵Group coverage is defined as the lowest coverage rate among all the groups.

Table 6: Comparison of group coverage between VCP and PT-VCP on regression tasks across different datasets ($\alpha = 0.1$).

Dataset	Group	VCP	PT-VCP
bike	Day	0.878 ± 0.007	0.884 ± 0.010
	Month	0.826 ± 0.010	0.857 ± 0.011
	Year	0.851 ± 0.005	0.871 ± 0.004
star	Gender	0.905 ± 0.008	0.905 ± 0.002
	Stark	0.890 ± 0.005	0.895 ± 0.007
	School1	0.902 ± 0.008	0.899 ± 0.022
meps-19	SEX=1	0.883 ± 0.004	0.895 ± 0.001
	MARRY=1	0.901 ± 0.004	0.901 ± 0.003
	REGION=1	0.862 ± 0.005	0.877 ± 0.006
meps-20	FTSTU=1	0.893 ± 0.004	0.900 ± 0.002
	ACTDTY=1	0.897 ± 0.003	0.902 ± 0.002
	HONRDC=1	0.792 ± 0.010	0.846 ± 0.008
meps-21	RTHLTH=1	0.864 ± 0.004	0.877 ± 0.004
	MNHLTH=1	0.856 ± 0.004	0.873 ± 0.004
	HIBPDX=1	0.755 ± 0.013	0.818 ± 0.009

D Experiment Details

In this section, we provide implementation details of the experiments in this paper, including experiments on synthetic datasets in Appendix D.1 and experiments on real-world datasets in Appendix D.2.

D.1 Synthetic Datasets

This section presents experiment details about the motivating example (Section 3.2) in Appendix D.1.1 and failure case (Section 3.4) in Appendix D.1.2.

D.1.1 Motivating Example

In our motivating example, we consider a simple data-generating process where the true underlying model is linear with Gaussian mixture noise:

$$Y = \mathbf{X}^\top \boldsymbol{\beta} + \epsilon, \quad \mathbf{X} \sim \mathcal{N}(\mathbf{0}, I_2).$$

The noise term ϵ follows $\mathcal{N}(\mu, 1)$ with probability 0.5 and $\mathcal{N}(-\mu, 1)$ with probability 0.5. The training, calibration, and test folds are all generated from this distribution. To emulate model misspecification, we fit the training fold using a linear model with Gaussian noise. Throughout the experiments, we set $\mu = 20$, $\alpha \in \{0.1, 0.2\}$, and $p \in \{0.96, 0.98\}$. We further average results over 5 random seeds and report the corresponding standard errors. Both VCP (Algorithm 2) and PT-VCP are evaluated under this setting.

Table 7: Comparison between CQR and PT-CQR regarding interval stability.

Dataset	CQR	PT-CQR
meps-19	0.00 ± 0.000	0.13 ± 0.005
meps-20	0.00 ± 0.000	0.13 ± 0.006
meps-21	0.00 ± 0.000	0.14 ± 0.003
bike	0.00 ± 0.000	0.08 ± 0.001
blog-data	0.00 ± 0.000	0.11 ± 0.003
bio	0.00 ± 0.000	0.10 ± 0.000
facebook-1	0.00 ± 0.000	0.10 ± 0.001
facebook-2	0.00 ± 0.000	0.10 ± 0.001
concrete	0.00 ± 0.000	0.13 ± 0.002
star	0.00 ± 0.000	0.12 ± 0.001

Table 8: Comparison between VCP and PT-VCP in classification tasks regarding interval stability. Experiments on RAPS ($\alpha = 0.1, p = 0.95$), with index range chosen as 300.

MODEL	BIAS	VCP	PT-VCP
RESNET18	40	0.02 ± 0.004	12.08 ± 0.060
RESNET50	40	0.07 ± 0.017	11.86 ± 0.057
RESNET101	40	0.01 ± 0.004	11.93 ± 0.089
RESNET152	40	0.19 ± 0.002	11.91 ± 0.058
RESNEXT101	40	0.20 ± 0.000	11.89 ± 0.083
VGG16	40	0.11 ± 0.030	12.00 ± 0.060
SHUFFLENET	40	0.03 ± 0.025	12.08 ± 0.055
INCEPTION	40	0.07 ± 0.010	12.19 ± 0.080
DENSENET161	40	0.03 ± 0.006	11.90 ± 0.057

D.1.2 Failure Case

In Figure 5, we present a failure case where VCP outperforms PT-VCP. Here, we modify the data-generating process to a linear model with Gaussian noise and fit it with the same linear model, so that no model misspecification arises in contrast to our motivating example. In this setting, the distribution of the score function fails to satisfy the sufficient condition in Corollary 3, which explains why VCP outperforms PT-VCP.

D.2 Real World Datasets

In this section, we firstly introduce the model structure in our experiments in Appendix D.2.1. Then we present the experiment details, including experiments on marginal and group coverage (Appendix D.2.2, Appendix D.2.6), regression tasks (Appendix D.2.3), classification tasks (Appendix D.2.4), ablation studies (Appendix D.2.5) and interval stability (Appendix D.2.7).

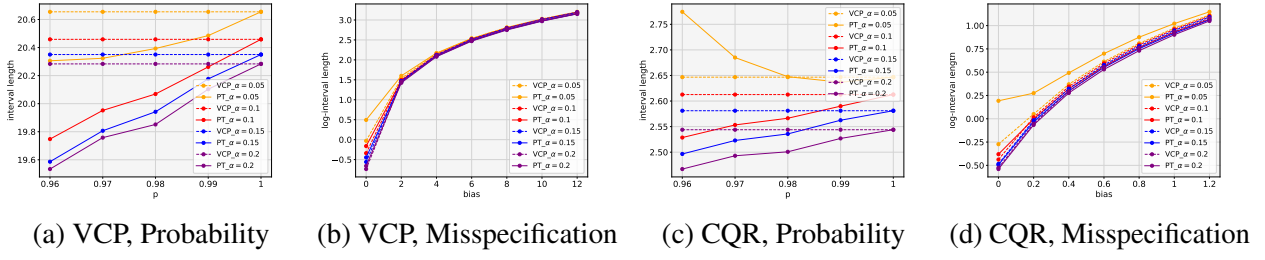


Figure 6: Ablation studies of dataset BIKE on different misspecification levels (b, d) and probability hyperparameters (a, c), including comparisons with VCP (a–b) and CQR (c–d).

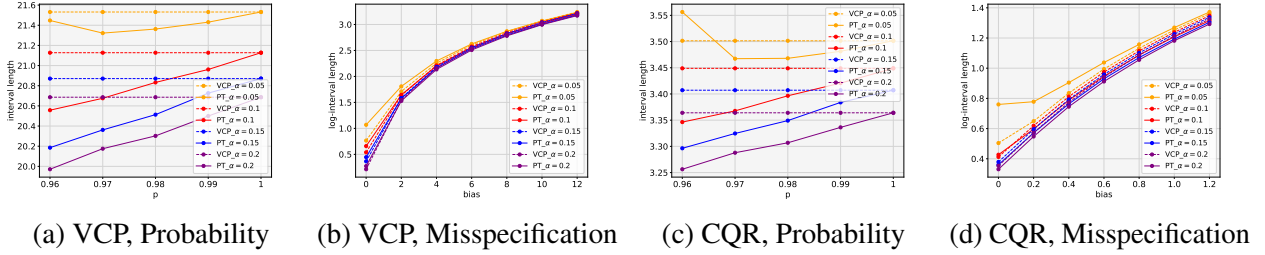


Figure 7: Ablation studies of dataset BIO on different misspecification level (a, c) and probability hyperparameter (b, d), including the comparison with VCP (a-b) and CQR (c-d).

D.2.1 Model Structure

In this section, we present the details of the structure of our model on real world datasets. Specifically, our model shares the same structure with (Romano et al., 2019).

Neural Net. Our neural network design includes three fully connected layers, with ReLU activation functions applied between each layer. The initial layer accepts an input feature vector X of n dimensions and produces 64 hidden units. The second layer mirrors this structure, generating another set of 64 hidden units. The final layer is a linear output layer that provides a pointwise prediction for the response variable Y . The network’s parameters are optimized by minimizing a quadratic loss function. We used the Adam optimization algorithm with a constant learning rate of 5×10^{-4} , minibatch size of 64, and a weight decay coefficient of 10^{-6} . In addition, regularization of dropout is implemented, with a retention probability of 0.1 for hidden units. To avoid overfitting, early stop is used and the number of training epochs is determined by cross-validation, with a maximum cap of 1000 epochs.

CQR Neural Net. We utilize neural networks to implement CQR for quantile regression. The network structure is consistent with the one described above, with the sole difference being that the output of the quantile regression network is a two-dimensional vector, which indicates the lower and upper conditional quantiles. Additionally, the training process remains the same, except that the pinball loss function in equation is employed instead of the quadratic loss.

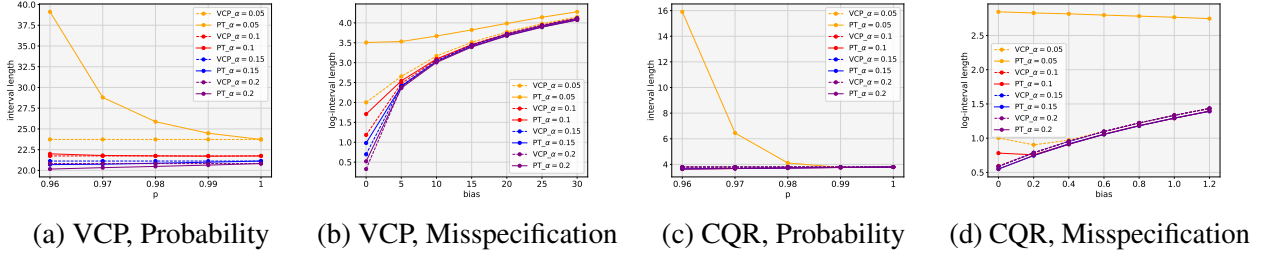


Figure 8: Ablation studies of dataset BLOGDATA on different misspecification level (a, c) and probability hyperparameter (b, d), including the comparison with VCP (a-b) and CQR (c-d).

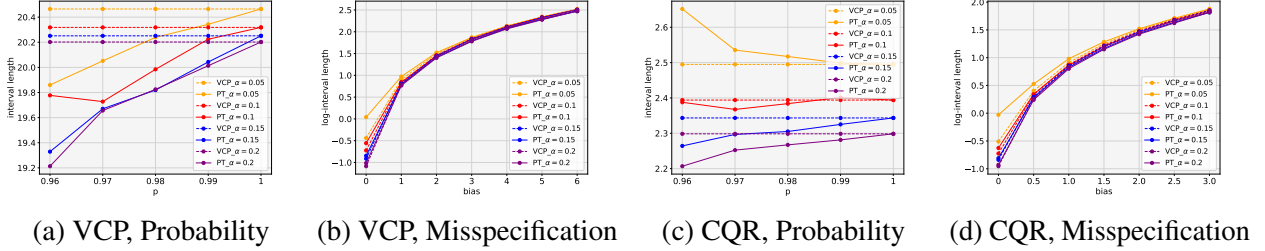


Figure 9: Ablation studies of dataset CONCRETE on different misspecification level (a, c) and probability hyperparameter (b, d), including the comparison with VCP (a-b) and CQR (c-d).

D.2.2 Marginal and Group Coverage

In Figure 1, we compare the coverage of VCP and PT-VCP on the BIKE dataset (Fanaee-T, 2013). Specifically, we evaluate several choices of α and p , and report both the marginal coverage and the group coverage (an empirical indicator of conditional coverage). The group coverage is obtained by partitioning the data according to Day, Month, and Year.

D.2.3 Regression Tasks

In ordinary regression tasks, we employ the neural network described in Section D.2.1 to fit several real-world datasets: MEPS19–21 (Cohen et al., 2009), BIKE (Fanaee-T, 2013), BLOG-DATA (Buza, 2014), BIO (Rana, 2013), FACEBOOK1–2 (Singh, 2015), CONCRETE (Yeh, 1998), and STAR (Achilles et al., 2008). To mimic model misspecification, we introduce a bias term that is directly added to the logits output by the neural network. The magnitude of this bias term, which varies across datasets, is reported in Table 2. Throughout these experiments, we set $\alpha = 0.1$ and $p = 0.95$, under which both VCP (Algorithm 2) and PT-VCP are evaluated. We further average results over 5 random seeds and report the corresponding standard errors.

In CQR tasks, we employ the CQR neural network described in Section D.2.1 to fit several real-world datasets: MEPS19–21 (Cohen et al., 2009), BIKE (Fanaee-T, 2013), BLOG-DATA (Buza, 2014), BIO (Rana, 2013), FACEBOOK1–2 (Singh, 2015), CONCRETE (Yeh, 1998), and STAR (Achilles et al., 2008). To mimic model misspecification, we introduce a bias term by directly adding it to both the lower and upper quantiles estimated by the quantile regression. The magnitude of this bias varies across datasets. Throughout the experiments, we set $\alpha = 1$ and $p = 0.95$, under which both

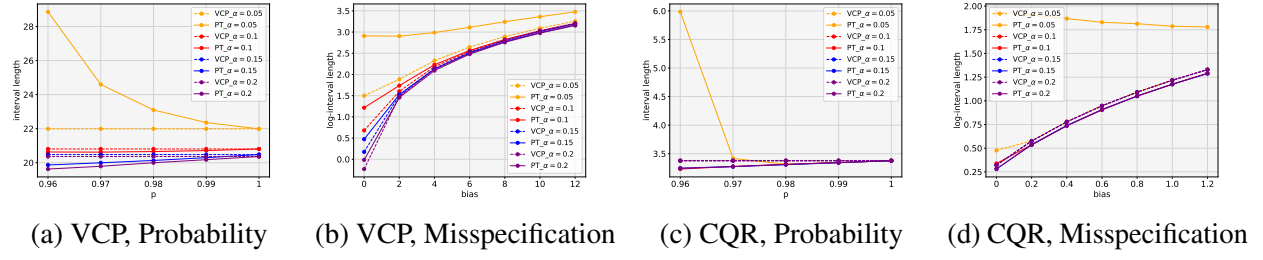


Figure 10: Ablation studies of dataset FACEBOOK1 on different misspecification level (a, c) and probability hyperparameter (b, d), including the comparison with VCP (a-b) and CQR (c-d).

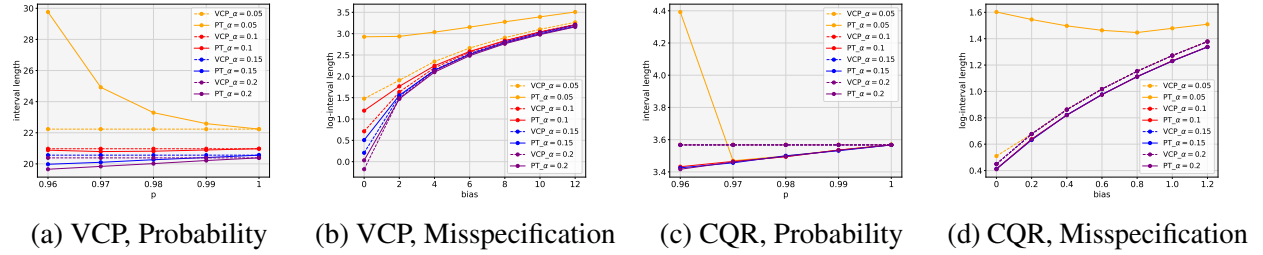


Figure 11: Ablation studies of dataset FACEBOOK2 on different misspecification level (a, c) and probability hyperparameter (b, d), including the comparison with VCP (a-b) and CQR (c-d).

CQR and PT-CQR are evaluated, as reported in Table 5. We further average results over 5 random seeds and report the corresponding standard errors.

D.2.4 Classification Task

In classification tasks, we apply PT to the real-world IMAGENET-VAL dataset (Deng et al., 2009) using several pre-trained models listed in Table 4, following a setting similar to Angelopoulos et al. (2020). To simulate model misspecification, we introduce a bias to the logits of several classes before the softmax operation. The magnitude of this bias is scaled according to the outputs, and the number of biased classes is specified by an index range in our experiments. For the classification task, we adopt RAPS (Angelopoulos et al., 2020) as the score function and set $\alpha = 0.1$ and $p = 0.95$. We further average results over 5 random seeds and report the corresponding standard errors.

D.2.5 Ablation Studies

The ablation studies mainly focus on regression tasks, including both ordinary regression and CQR. We conduct experiments on all datasets used in the regression setting. For these ablation studies, we set $\alpha \in \{0.05, 0.1, 0.15, 0.2\}$, $p \in \{0.96, 0.97, 0.98, 0.99, 1.00\}$, and apply dataset-specific bias magnitudes.

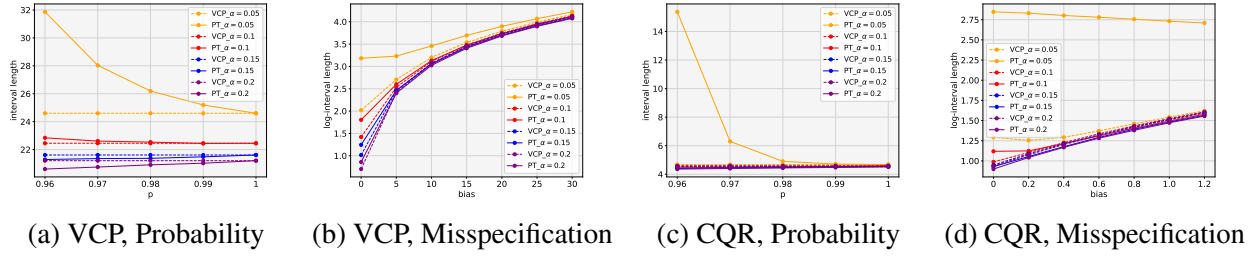


Figure 12: Ablation studies of dataset MEPS19 on different misspecification level (a, c) and probability hyperparameter (b, d), including the comparison with VCP (a-b) and CQR (c-d).

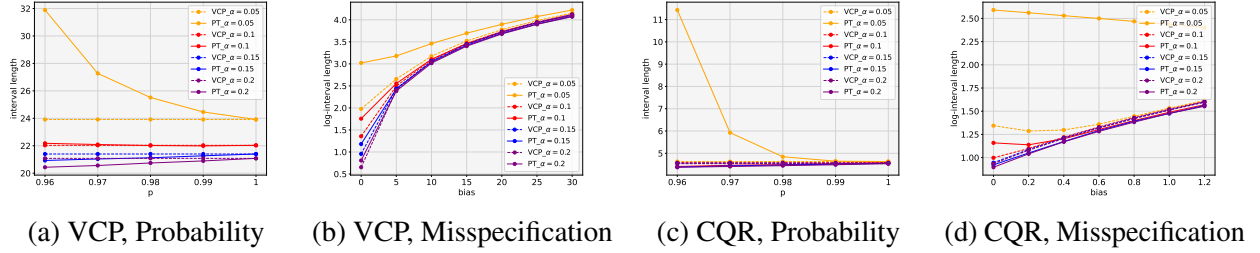


Figure 13: Ablation studies of dataset MEPS20 on different misspecification level (a, c) and probability hyperparameter (b, d), including the comparison with VCP (a-b) and CQR (c-d).

D.2.6 Group Coverage

To demonstrate that PT-VCP does not degrade conditional coverage compared to VCP, we conduct experiments measuring group coverage on the MEPS19–21 (Cohen et al., 2009), BIKE (Fanaee-T, 2013), and STAR (Achilles et al., 2008) datasets. The grouping strategies are summarized in Table 6. In these experiments, we set $\alpha = 0.1$ and $p = 0.95$, and further average results over 5 random seeds, reporting the corresponding standard errors.

D.2.7 Interval Stability

To compare the newly proposed metric *interval stability* between VCP and PT-VCP, we conduct experiments on both regression and classification tasks, using different datasets and pre-trained models, respectively. The results are reported in Table 3, Table 7, and Table 8. We measure *interval stability* by computing the variance of the interval (or set) length (or size) for repeated predictions on the same input, and then averaging this variance over all inputs X . Results are further averaged over 5 random seeds, with the corresponding standard errors reported.

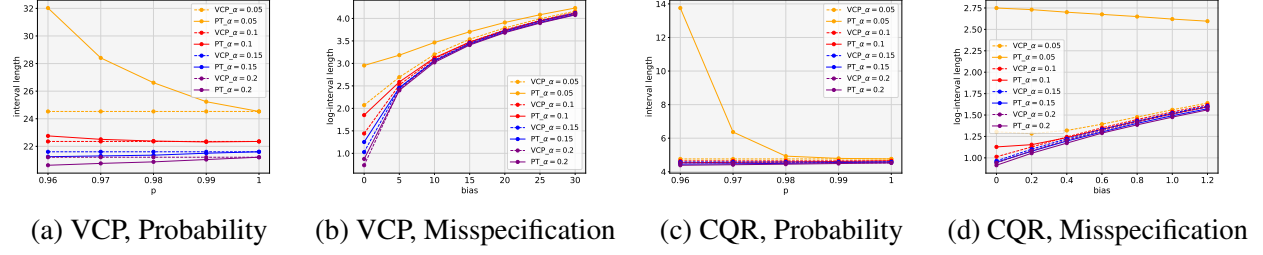


Figure 14: Ablation studies of dataset MEPS21 on different misspecification level (a, c) and probability hyperparameter (b, d), including the comparison with VCP (a-b) and CQR (c-d).

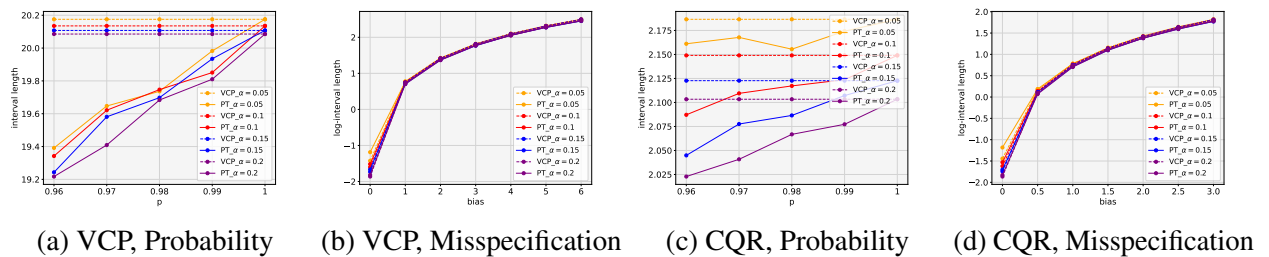


Figure 15: Ablation studies of dataset STAR on different misspecification level (a, c) and probability hyperparameter (b, d), including the comparison with VCP (a-b) and CQR (c-d).